(MeO-PEG-NH_2, Mw = 12 kg/mol) were obtained from Nippon Oil and Fats, Co., Ltd. (Tokyo, Japan). Amine reagents used in aminolysis reaction were purchased from Tokyo Kasei Kogyo, Co., Ltd. (Tokyo, Japan). Chemicals for dendrimer synthesis were purchased from Tokyo Kasei Kogyo and Sigma Aldrich, Co. Inc (St. Louis, MO). *n*-Pentanol and 1,8-diazabicyclo-(5,4,0)-undec-7-ene (DBU) were purchased from Tokyo Kasei Kogyo, and used without further purification. All solvents for the polymer synthesis were distilled before use.

2.1.1. Synthesis of polymers

PEG-*block*-poly(β-benzyl-L-aspartate) (PEG-*b*-PBLA) was prepared according to the previously reported method [20]. PEG-*b*-polyaspartatamide catiomers carrying ethylenediamine repeating units at the side chain were prepared through the quantitative aminolysis reaction of PEG-*b*-PBLA in dry DMF at 40 °C for 24 h in the presence of 50-fold molar of ethylenediamine (EDA), diethylenetriamine (DET), triethylenetetramine (TET) and tetraethylenepentamine (TEP) according to the previously reported method [20]. The details of the synthetic procedures and the confirmation of the chemical structures of the synthesized PEG-*b*-polycation copolymers are shown in Figs. S1, S2, S3, S4, S5 and Table S1 in Supporting information.

Synthesis of ionic dendrimer phthalocyanine (DPc) was performed according to the method reported by Ng's group [21]. The second generation of dendritic phenol was reacted with 4-nitrophthalonitrile by an alkali-mediated coupling reaction to obtain the corresponding dendritic phthalonitrile, which was then treated with Zn $(OAc)_2$ and DBU in *n*-pentanol to give the dendrimer phthalocyanine. The dendrimer phthalocyanine thus obtained was treated with a THF/H_2O mixture solution containing NaOH to obtain ionic dendrimer phthalocyanine (DPc; Mw: 4904). The chemical structure of DPc was shown in Fig. 2c.

2.1.2. Preparation of DPc-incorporated polyion complex

The given amount of DPc and PEG-*b*-PLL (Mw of PEG = 12,000, repeating unit of PLL = 49) (Fig. 2b) was separately dissolved in NaH_2PO_4 (10 mM, pH 4.81 and Na_2HPO_4 (10 mM, pH 9.20) solutions, respectively, and then mixed at a stoichiometric ratio to give a final concentration of DPc 1 mg/ml [22]. The resulting micelle is spherical, with a diameter of ca. 50 nm and narrow size distribution [22].

2.1.3. Preparation of pDNA-incorporated polyplex micelles

Block copolymer and plasmid pCAcc+Luc (pDNA) [23] were dissolved separately in 10 mM Tris–HCl buffer (pH 7.4). Then, polymer solution was added to pDNA solution at a fixed concentration (50 μg/ml) to form complex with various N/P ratios. N/P ratio is defined as the ratio of molar concentration of cationic moieties in diblock catiomer to that of phosphate group in pDNA. Final concentration of pDNA was fixed at 33.3 μg/ml. Complexes were kept at room temperature overnight before use.

2.1.4. Dynamic light scattering measurement

The size of pDNA polyplex micelles was evaluated by dynamic light scattering (DLS) measurement. Sample solutions

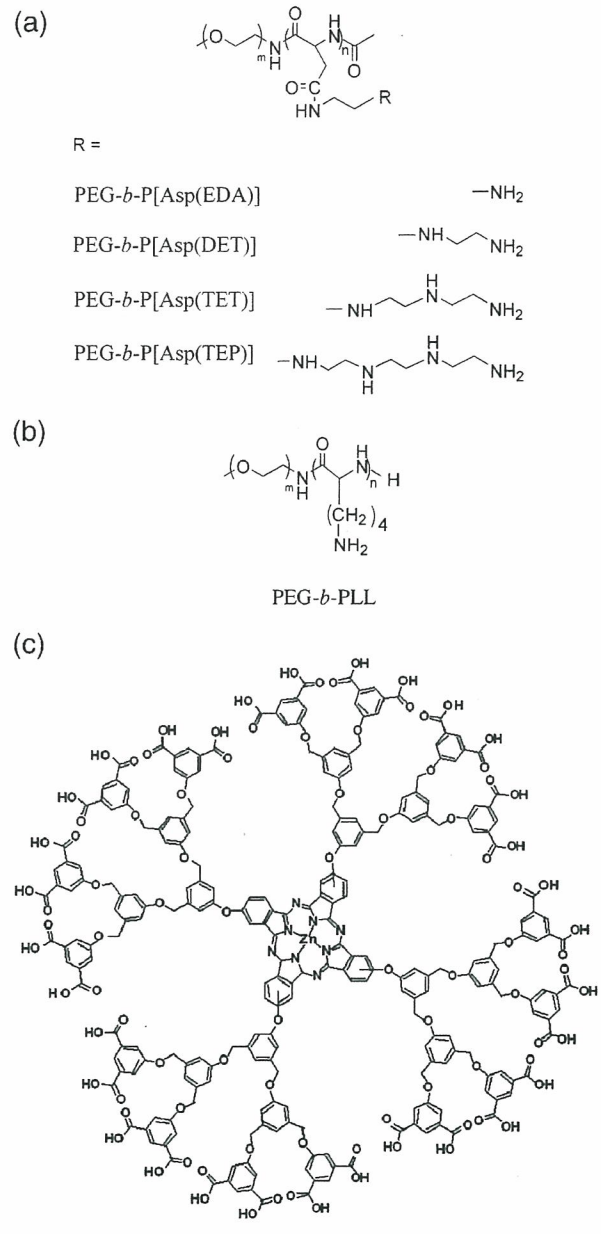

Fig. 2. (a) Chemical structures of PEG-*b*-P[Asp(EDA)], PEG-*b*-P[Asp(DET)], PEG-*b*-P[Asp(TET)], and PEG-*b*-P[Asp(TEP)]; (b) chemical structure of PEG-*b*-PLL; (c) chemical structure of anionic dendrimer phthalocyanine (DPc).

with various N/P ratios in 10 mM Tris–HCl buffer (pH 7.4) were adjusted to pDNA concentration of 33.3 μg/ml. DLS measurements were carried out at 25.0±0.2 °C using a DLS-7000 instrument (Otsuka Electronics, Osaka, Japan) with a vertically polarized incident beam of 488 nm wavelength from an Ar ion laser. A scattering angle of 90° was used in these measurements. Data were analyzed by a cumulant method as reported in detail previously [24].

2.1.5. Laser-doppler electrophoresis measurement

Laser-doppler electrophoresis measurements were carried out using a ELS-6000 (Otsuka Electronics Co., Ltd., Osaka, Japan) at 25 °C. From the electrophoretic mobility, the zeta

potential (ζ) was calculated using Smoluchowski equation as follows:

$$\zeta = 4\pi\eta u/\varepsilon$$

where u is the electrophoretic mobility, η is the viscosity of the solvent, and ε is the dielectric constant of the solvent.

2.1.6. Ethidium bromide exclusion assay

The effect of the N/P ratio on the degree of pDNA condensation in PIC micelle was estimated from the reduction in fluorescence intensity of ethidium bromide (EtBr) due to the exclusion from DNA. PIC micelle solutions (33.3 μg of pDNA/mL) prepared at various N/P ratios were adjusted to 20 μg of pDNA/mL with 0.4 μg of EtBr/mL by adding 10 mM Tris–HCl buffer containing EtBr. The ratio of residual molar concentration of EtBr to that of the base pair in pDNA was 0.033. The solutions were incubated at ambient temperature overnight. Fluorescence measurement of sample solution was carried out at 25±0.2 °C using a spectrofluorometer (JASCO, FP-6500). Excitation (Ex) and emission (Em) wavelengths were 510 and 590 nm, respectively. Results were expressed as relative fluorescence intensity. The fluorescence of pDNA solution with EtBr was set at 100%, and measured against a background of EtBr without pDNA.

2.1.7. Cell culture and photochemical transfection

Human hepatoma Huh7 cells were cultured in DMEM containing 10% fetal bovine serum (FBS) and 10 mM HEPES buffer. The cells were grown at 37 °C in humidified atmosphere containing 5% CO_2. In the experiment, 10,000 cells per well were plated on 24-well plate 24 h before transfection. The cells then were incubated in a medium containing DPc-loaded micelles and pDNA polyplex micelles prepared at an N/P ratio of 2. The amount of pDNA was adjusted to 1 μg per well while DPc concentrations were varied. After 6 h incubation at 37 °C, the medium was replaced with fresh medium to remove non-associated photosensitizers. The cells then were irradiated for 45 min (except for irradiation times variation experiment) using halogen lamp equipped with a band-pass filter (400–700 nm) at a fluence rate of 3 mW/cm^2. After another 48 h incubation at 37 °C, the luciferase gene expression was measured using LB940, Berthold Technologies (Bad Wilbad, Germany). The amount of protein in each well was determined using Micro BCA Protein Assay Reagent Kit, Pierce Chemical Co., Inc. (Rockford, USA).

2.1.8. Cytotoxicity measurement

Cell culture was carried out as described above. After 48 h incubation, the viability of the cells was evaluated using 3-(4,5-dimethylthiazol-2-yl)-2,5-diphenyltetrazolium bromide (MTT) assay [25]. Briefly, 40 μl of MTT solution (5 mg/ml in PBS) was added to each well, followed by 4 h incubation at 37 °C. Then, 400 μl SDS solution (20% w/v in PBS) was added to dissolve the formed formazan. After 2 days incubation at room temperature, the absorbance from each well was measured at 570 nm. Results were expressed as percentage relative to control.

3. Results and discussion

The PEG-*b*-polyaspartatamide catiomers with different amino functionality at the side chain used for pDNA delivery were synthesized through the new synthetic procedure of PEG-*b*-polycatiomer developed in our laboratory [20]. It based on the recent finding that the benzyl ester group of poly(β-benzyl-L-aspartate) (PBLA) can undergo aminolysis reaction with the primary amino group of polyamine compounds in a selective and quantitative manner under a mild condition, allowing the preparation of cationic polyaspartatamides with different amino functionality but the same molecular weight. In our previous study, we found that PEG-*b*-polycatiomer having the ethylenediamine structure at the side chain showed sufficient buffering

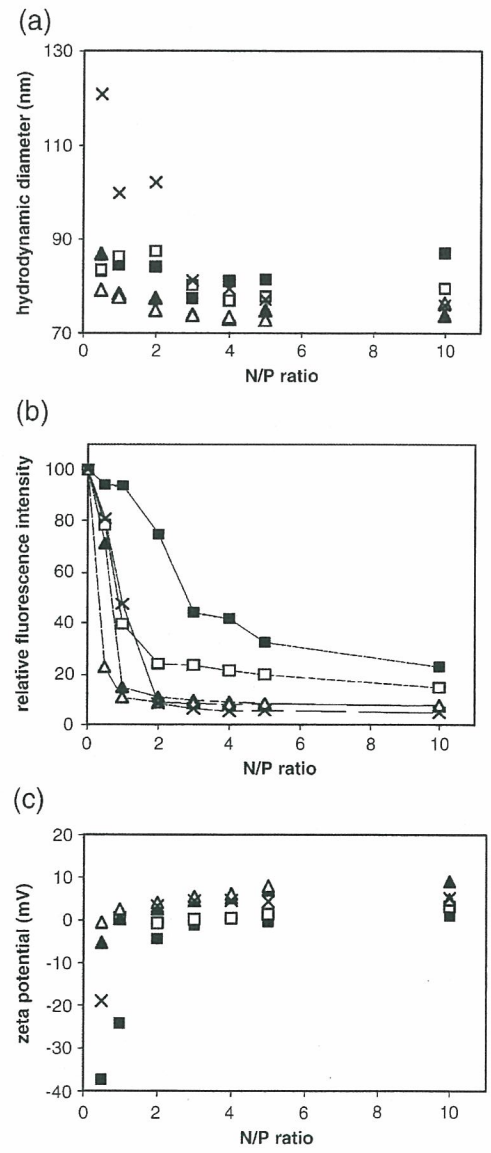

Fig. 3. Properties of PEG-*b*-polycation/pDNA polyplex micelles: (a) change in the cumulant diameter, (b) fluorescence intensity of EtBr and (c) zeta potential value of the polyplexes prepared at different mixing ratios. (■) PEG-*b*-P[Asp(EDA)]; (□) PEG-*b*-P[Asp(DET)]; (▲) PEG-*b*-P[Asp(TET)]; (△) PEG-*b*-P[Asp(TEP)]; (×) PEG-PLL.

capacity and therefore enhanced transfection efficiency based on the aforementioned proton sponge effect [20]. In this study, we hypothesized that the use of the buffering polycations might facilitate the PCI-mediated gene delivery, and aimed to optimize the chemical structure of PEG-*b*-polycatiomers for this purpose. Therefore, we synthesized a series of PEG-*b*-polycatiomers carrying the ethylenediamine repeating units (PEG-*b*-P[Asp (EDA)]), PEG-*b*-P[Asp(DET)], PEG-*b*-P[Asp(TET)] and PEG-*b*-P[Asp(TEP)]) at the side chain with fixed composition of 12–68 (Mw of PEG=12,000, repeating unit of cationic segment=68). The chemical structures of these block catiomers were confirmed by ^{1}H NMR and size exclusion chromatography measurements (Figs. S1, S2, S3, S4, S5 and Table S1 in Supporting information), and are shown in Fig. 2a.

The polyplex micelles were prepared by mixing the solution of each polymer and pDNA at various N/P ratios. The size of the polyplexes was then evaluated by DLS measurement. The hydrodynamic diameter of the polyplexes was revealed to be 70–90 nm through the range of examined N/P ratios as shown in Fig. 3a. Increasing N/P ratio decreases the hydrodynamic diameter of the polyplexes, suggesting the formation of more compact pDNA micelles probably due to the increased densities of positive charges surrounding pDNA polyplexes. From the practical point of view, the polyplex micelles need to be stable under physiological salt concentrations. Therefore, the DLS measurements of the polyplex micelles were carried out after 24-h incubation in 150 mM NaCl solutions. Consequently, the polyplex micelles maintained the particle size of 100 nm with a narrow distribution above the N/P ratio of 2.0, whereas the branched polyethylenimine (BPEI) polyplexes showed appreciable increases in the particle size and polydispersity index (Fig. S6 in Supporting information). This result suggests high stability of polyplex micelles under physiological conditions for *in vivo* use.

Ethidium bromide (EtBr) is a DNA intercalator and exhibits approximately 10-fold greater fluorescence emission upon binding to DNA. Condensation of DNA by cationic component displaces EtBr, resulting in the reduced fluorescence intensity. Hence, EtBr exclusion assay was frequently used to estimate the degree of pDNA condensation in polyplexes [26]. We found that in the order of PEG-*b*-P[Asp(EDA)], PEG-*b*-P[Asp(DET)], PEG-*b*-P[Asp(TET)] and PEG-*b*-P[Asp(TEP)], pDNA condensation ability increased (i.e., the N/P ratio required to reduce the EtBr fluorescent intensity decreased) as shown in Fig. 3b. It seems that longer polyamine side chain more effectively interacts with DNA double strands, thereby replacing the dye molecule. Except for PEG-*b*-P[Asp(EDA)], all the PEG-*b*-polycatiomers induced EtBr quenching to be leveled off at N/P ratio of 2, suggesting the completion of pDNA condensation at N/P ratio less than 2. PEG-*b*-P[Asp(EDA)]/pDNA polyplex retained 75% of its fluorescence intensity at N/P ratio of 2. As known, P[Asp(EDA)] has shorter spacer between the primary amino group and backbone polymer, and this may explain the lower condensation ability of DNA.

Zeta potential values of the polyplex micelles increased with increasing N/P ratio and were almost leveled off at N/P ratio of 2 (Fig. 3c). EtBr exclusion assay also indicated that at N/P ratio

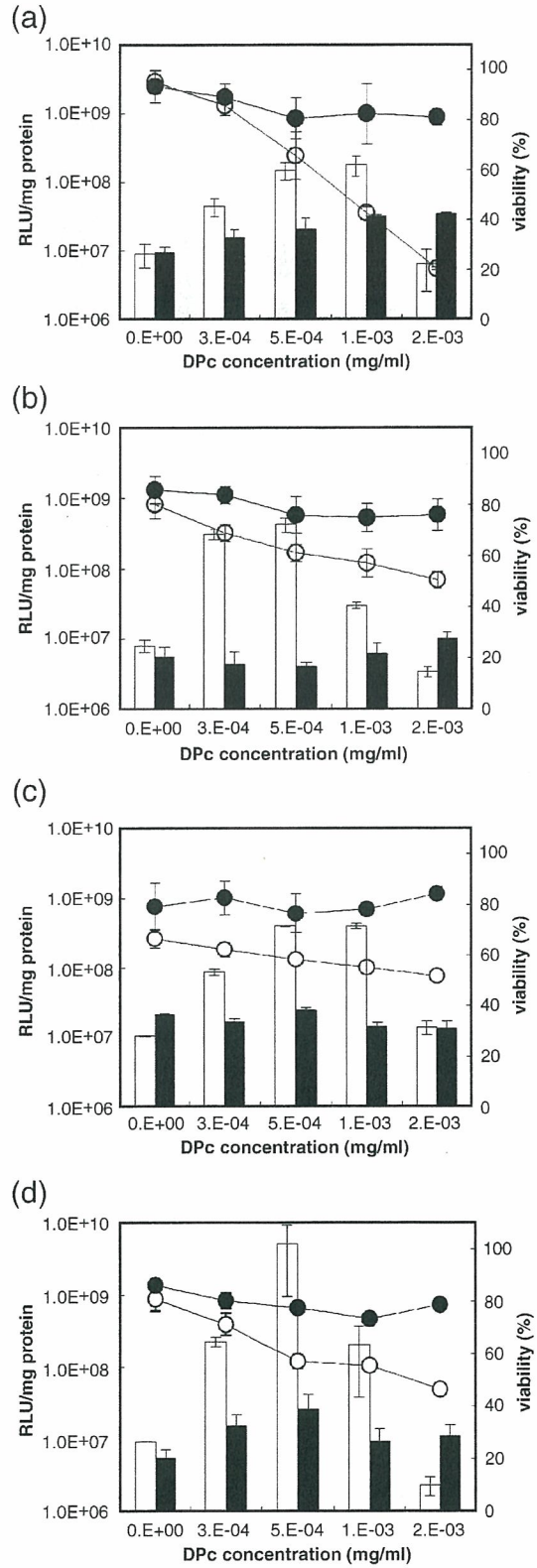

Fig. 4. The effect of DPc concentration on the transfection efficiency and cytotoxicity of the PCI-mediated transfection using the combination of pDNA- and DPc-incorporated micelles. (a) PEG-*b*-P[Asp(EDA)], (b) PEG-*b*-P[Asp (DET)], (c) PEG-*b*-P[Asp(TET)] and (d) PEG-*b*-P[Asp(TEP)] as pDNA vector. Open bar: transfection efficiency with irradiation; solid bar: transfection efficiency without irradiation; ○: photocytotoxicity; ●: dark cytotoxicity.

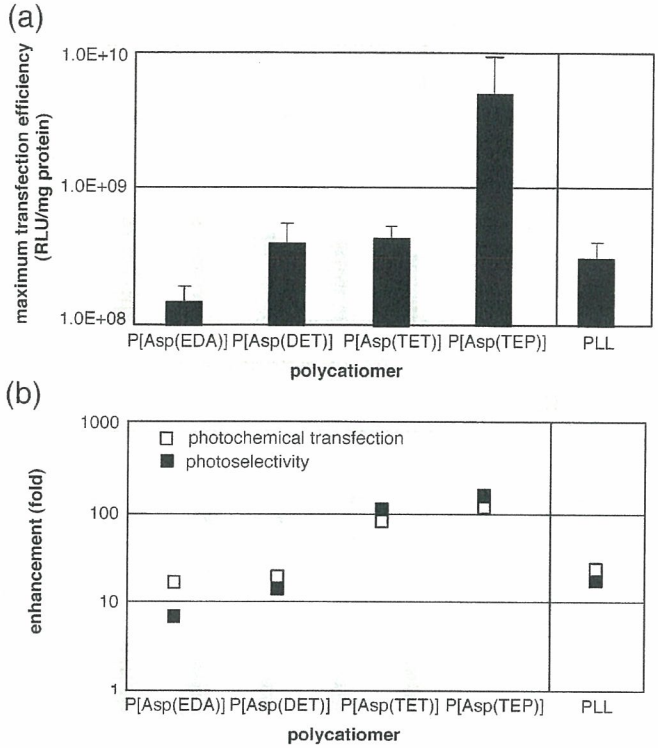

Fig. 5. Comparison of (a) transfection efficiency and (b) photochemical transfection enhancement and photoselectivity at optimal DPc concentration between the polyplex micelles from PEG-*b*-P[Asp(EDA)], PEG-*b*-P[Asp (DET)], PEG-*b*-P[Asp(TET)], PEG-*b*-P[Asp(TEP)] and PEG-*b*-PLL.

of 2, the pDNA was fully condensed in the core. A gradual increase of the zeta potential suggests adsorption of polymer onto the polyplex surface. Above N/P ratio of 2, the polyplexes have relatively small absolute zeta potential values, suggesting the formation of the core-shell structured polyplex micelles covered with PEG palisades. The sterically repulsive character of the neutral PEG layers prevents the micelles from secondary aggregation, keeping their highly dispersive nature in aqueous medium. These characters are expected to provide the polyplexes with prolonged blood circulation by avoiding interaction with serum proteins and cellular components [17]. Another advantage of the presence of neutral PEG layers at the outer part of the micelle might be the minimization of toxicity of the polycatiomers due to its binding with various types of RNA and genomic DNA that impairs the normal cellular functions of these polyanions [27].

In this study, the PCI using polymeric micelles incorporating dendrimer-based photosensitizers [dendrimer phthalocyanine (DPc) illustrated in Fig. 2c] was carried out to enhance the gene transferring ability of the aforementioned polyplex micelles in a light-selective manner. DPc has longer excitation wavelengths (i.e., strong Q-band absorptions at 630 and 685 nm), facilitating deeper tissue penetration of light therefore preferable for clinical use [28,22]. The rationale for the use of polymeric micelles as a nanocarrier of DPc is similar to that for the delivery of DNA, which are to prolong blood circulation after intravenous administration and to selectively accumulate them in the target tissues such as solid tumors as previously reported [22,29,30]. Also, both micelles are assumed to show the same subcellular localization in the endosome due to similar particle sizes and surface properties, which might be a key to success in the PCI-mediated gene delivery [14,19].

To evaluate the ability of the combinatorial use of the newly developed polyplex micelles and DPc-incorporated micelles for the PCI-mediated gene delivery, *in vitro* transfection was performed on human hepatoma Huh7 cells with a luciferase (Luc) reporter gene in the presence and absence of photoirradiation. The photochemical transfection and cytotoxicity were examined using the combination of polyplex micelles at N/P ratio of 2, where the fluorescence intensity was found to be leveled off for most of the complexes (Fig. 3b), and the DPc-incorporated micelles with different concentrations of DPc. The photoirradiation was carried out using a broad band light of 400–700 nm with 3 mW/cm^2 of fluence rate for 45 min. The PCI-mediated gene transferring ability and cytotoxicity of the polyplexes from PEG-*b*-P[Asp(EDA)], PEG-*b*-P[Asp(DET)], PEG-*b*-P[Asp(TET)] and PEG-*b*-P[Asp(TEP)] are shown in Fig. 4a, b, c and d, respectively. All the polyplexes showed the photochemical enhancement of the gene expression with optimum doses of DPc ($5*10^{-4}$ mg/ml), above in which the transfection efficiency decreased. The decrease of transfection efficiency with increasing DPc concentration is most likely to be caused by increased photocytotoxicity (open symbols in Fig. 4). Hence, the PCI-mediated transfection with the DPc-incorporated micelles should be performed based on a careful balance between transfection efficiency and cytotoxicity. But there is also another possibility that the lowered transfection may be due to the damage of the plasmid DNA induced by photochemical treatment [31].

The maximum transfection efficiencies achieved by the PCI-mediated gene delivery using polyplex micelles from different block catiomers are summarized in Fig. 5a. Also, the photochemical transfection enhancement and photoselectivity are shown in Fig. 5b. Photochemical transfection enhancement is defined as the ratios of the above-mentioned maximum transfection efficiency to the transfection efficiency of the polyplex

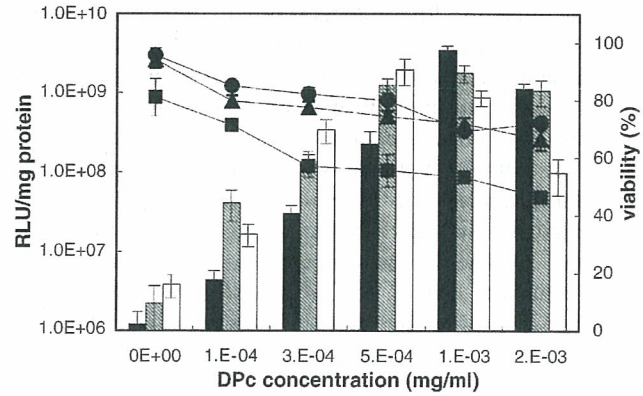

Fig. 6. The effect of irradiation times on photochemical transfection [solid bar: 20 min; hatched bar: 30 min; open bar: 45 min irradiation] and photocytotoxicity [●: 20 min; ▲: 30 min; ■: 45 min irradiation] of PEG-*b*-P[Asp(TEP)] polyplex micelle at different DPc concentrations.

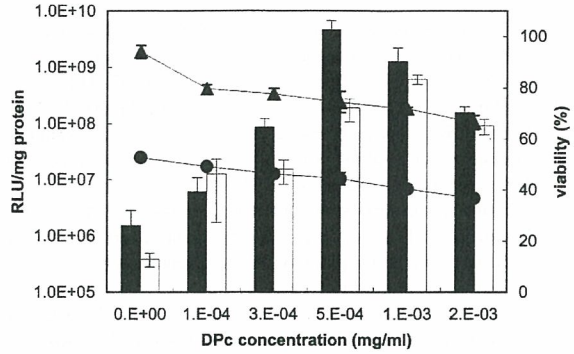

Fig. 7. Comparison of photochemical transfection efficiency (solid bar: BPEI; open bar: PEG-*b*-P[Asp(TEP)]) and photocytotoxicity (●: BPEI; ▲: PEG-*b*-P[Asp(TEP)]) between the polyplex micelles from PEG-*b*-P[Asp(TEP)] and BPEI 25 kDa at various concentrations of DPc and 20 min irradiation.

micelles alone, while photoselectivity is the ratios of the maximum PCI-mediated transfection efficiency to the transfection efficiency of the combination of the pDNA- and DPc-incorporated micelles without photoirradiation. As shown in Fig. 5a, increasing the length of ethylenediamine structure at the side chain of polycation segment of diblock copolymer led to an appreciable increase in the photochemical transfection efficiency even at the same N/P ratio. Also, the polyplexes from PEG-*b*-polyaspartatamide catiomer gave a higher photochemical transfection than those of PEG-*b*-PLL, except for PEG-*b*-P[Asp(EDA)], which lacks both the ability to condense DNA and buffering capacity [20]. Notably, PEG-*b*-P[Asp(TEP)] bearing 3 times-repeated ethylenediamine units showed a 1000-fold photochemical transfection enhancement, which is in a marked contrast with those obtained by PEG-*b*-P[Asp(TET)] bearing 2 times-repeated ethylenediamine units (76-fold) and PEG-*b*-P[Asp(DET)] bearing mono-ethylenediamine unit (19-fold) (Fig. 5b). Thus, the photochemical transfection enhancement of the polyplex micelles increased as the length of the ethylenediamine structure at the side chain of block catiomer strand increased. The mechanisms of the enhanced PCI-mediated transfection dependent on the length of the ethylenediamine side chain remain to be clarified. It is possible that the increasing number of a relatively low pK_a secondary amino groups may contribute to such transfection enhancement. Increasing the length of the ethylenediamine side chain increased the pDNA condensation ability (Fig. 3b), which may also contribute to the enhanced PCI-mediated transfection. However, this factor is unlikely to be solely effective in the photochemical transfection, since PEG-*b*-PLL showed lower PCI-mediated transfection efficiency than those of PEG-*b*-P[Asp(DET)], PEG-*b*-P[Asp(TET)] and PEG-*b*-P[Asp(TEP)] despite its high DNA condensation ability. Thus, as we hypothesized, the use of block catiomers having the ethylenediamine side chain with a high buffering capacity may assist the photochemical disruption of the endosomal membrane due to the proton sponge mechanism [5], thereby accelerating the cytoplasmic delivery of the polyplex micelles upon photoirradition. The synergistic effect between photochemical reaction and proton sponge effect on the PCI-mediated transfection has been successfully demonstrated in this study.

PEG-*b*-P[Asp(TEP)] gave the highest and remarkable photochemical transfection enhancement. In this experiment, the effect of the irradiation times on the PCI-mediated transfection using polyplex micelles from PEG-*b*-P[Asp(TEP)] was further studied. In particular, we tried to find an optimum irradiation condition for high transfection enhancement without a trade on the viability of the cells. Fig. 6 shows the photochemical transfection and photocytotoxicity of PEG-*b*-P[Asp(TEP)] polyplex micelle at different irradiation times. As the irradiation time increased, the optimum condition for photochemical transfection was shifted to a lower concentration of DPc while the photocytotoxicity increased. The highest photochemical transfection enhancement was achieved at DPc concentration of 0.001 mg/ml and irradiation times of 20 min with around 72% of the cells remained alive. Thus, this condition might be an optimum irradiation condition for photochemical transfection enhancement for PEG-*b*-P[Asp(TEP)] polyplex micelle.

Further, polyethylenimine (PEI) consisting of ethylenediamine units, which is one of the most highly transfectable polycatiomers, was used as pDNA vector for the PCI-mediated transfection. In this study, we compared the photochemical transfection efficiency and photocytotoxicity between PEG-*b*-P[Asp(TEP)] and 25 kDa branched PEI (BPEI) as pDNA vector (Fig. 7). BPEI showed approximately 7-fold higher transfection enhancement compared to PEG-*b*-P[Asp(TEP)] at the optimum DPc concentration. Nevertheless, the transfection with BPEI was accompanied by significant cytotoxicity. The PEG-*b*-P[Asp(TEP)] polyplex micelle showed significantly lower cytotoxicity despite its efficient PCI-mediated transfection ability.

In conclusion, we have studied on the relationship between chemical structure of block catiomers and photochemical transfection efficiencies. The light-inducible transfection activity was significantly enhanced as the length of the ethylenediamine side chain of PEG-*b*-polycatiomer increased. PEG-*b*-P[Asp(TEP)] gave the highest photochemical enhancement and photoselectivity of the transfection. The PEG-*b*-polyaspartatamide catiomers, except for PEG-*b*-P[Asp(EDA)], are more effective than PEG-*b*-PLL, which was used in the previous study [19], as a pDNA vector for the light-selected gene transfer. It is worth mentioning that all the polyplex micelles used in this study were prepared under the conditions with minimal free polymers (i.e., at the N/P ratio of 2.0), facilitating their use for the systemic administration. PEG-*b*-polyaspartatamide catiomers as pDNA vector might become vectors for the PCI-mediated gene transfer *in vivo* after systemic delivery.

Acknowledgments

The authors wish to express their gratefulness to the Health and Labor Sciences Research Grants in Research on Advanced Medical Technology in Nanomedicine Area from the Ministry of Health, Labor and Welfare (MHLW), Japan. Also, they wish to express their thanks to the Project on the Materials Development for Innovative Nano-Drug Delivery Systems from the Ministry of Education, Culture, Sports, Science and Technology (MEXT), Japan.

Appendix A. Supplementary data

Supplementary data associated with this article can be found, in the online version, at doi:10.1016/j.jconrel.2006.07.014.

References

[1] M.A. Kay, D.X. Liu, P.M. Hoogerbrugge, Gene therapy, Proc. Natl. Acad. Sci. 88 (1997) 5572–5576.

[2] I.M. Verma, N. Somia, Gene therapy—promises, problems and prospects, Nature 389 (1997) 239–242.

[3] W.F. Anderson, Human gene therapy, Nature 392 (1998) 25–30.

[4] D. Luo, W.M. Saltzman, Synthetic DNA delivery system, Nature 18 (2000) 33–37.

[5] O. Boussif, F. Lezoualc'h, M.A. Zanta, M.D. Mergny, D. Scherman, B. Demeneix, J.P. Behr, Versatile vector for gene and oligonucleotide transfer into cells in culture and in vivo: polyethylenimine, Proc. Natl. Acad. Sci. 92 (1995) 7297–7301.

[6] B. Abdallah, A. Hassan, C. Benoist, D. Goula, J.P. Behr, B.A. Demeneix, A powerful non-viral vector for in vivo gene transfer into the adult mammalian brain: polyethilenimine, Hum. Gene Ther. 7 (1996) 1947–1954.

[7] D. Fischer, T. Bieber, Y. Li, H.P. Elsasser, T. Kissel, A novel non viral vector for DNA delivery based on low molecular weight, branched polythylenimine: effect of molecular weight on transfection efficiency and cytotoxicity, Pharm. Res. 16 (1999) 1273–1279.

[8] S. Boeckle, K. von Gersdorff, S. van der Piepen, C. Culmsee, E. Wagner, M. Ogris, Purification of polyethylenimine polyplexes highlights the role of free polycations in gene transfer, J. Gene Med. 6 (2004) 1102–1111.

[9] P.K. Selbo, A. Høgste, L. Prasmickaite, K. Berg, Photochemical internalization: a novel drug delivery system, Tumor Biol. 23 (2002) 103–112.

[10] K. Berg, P.K. Selbo, L. Prasmickaite, T. Tjelle, K. Sandvig, J. Moan, G. Gaudernack, O. Fodstad, S. Kjolsrud, H. Anholt, G.H. Rodal, S. Rodal, A. Høgset, Photochemical internalization : a novel technology for delivery of macromolecules into cytosol, Cancer Res. 59 (1999) 1180–1183.

[11] A. Høgset, L. Prasmickaite, T.E. Tjelle, K. Berg, Photochemical transfection: a new technology for light-induced, site-directed gene delivery, Hum. Gene Ther. 11 (2000) 869–880.

[12] A. Høgset, L. Prasmickaite, P.K. Selbo, M. Hellum, B.Ø. Engesæter, A. Bondted, K. Berg, Photochemical internalization in drug and gene delivery, Adv. Drug Deliv. Rev. 56 (2004) 95–115.

[13] I.J. Macdonald, T.J. Dougherty, Basic principle of photodynamic therapy, J. Porphyr. Phthalocyanines 5 (2001) 105–129.

[14] N. Nishiyama, A. Iriyama, W.-D. Jang, K. Miyata, K. Itaka, Y. Inoue, H. Takahashi, Y. Yanagi, Y. Tamaki, H. Koyama, K. Kataoka, Light induced gene transfer from packaged enveloped in a dendrimeric photosensitizer, Nat. Matters 4 (2005) 934–941.

[15] Y. Takakura, H. Hashida, Macromolecular carrier systems for targeted drug delivery: pharmacokinetic considerations on biodistribution, Pharm. Res. 13 (1996) 820–831.

[16] K. Itaka, K. Yamauchi, A. Harada, K. Nakamura, H. Kawaguchi, K. Kataoka, Polyion complex micelles from plasmid DNA and poly(ethylene glycol)-poly(L-lysine) block copolymer as serum-tolerable polyplex system: physicochemical properties of micelles relevant to gene transfection efficiency, Biomaterials 24 (2003) 4495–4506.

[17] M. Harada-Shiba, K. Yamauchi, A. Harada, K. Shimokado, K. Kataoka, Polyion complex micelles as a vector for gene therapy-pharmacokinetics and in vivo gene transfer, Gene Ther. 9 (2002) 407–414.

[18] K. Miyata, Y. Kakizawa, N. Nishiyama, A. Harada, Y. Yamasaki, H. Koyama, K. Kataoka, Block catiomer polyplexes with regulated densities of charge and disulfide cross-linking directed enhance gene expression, J. Am. Chem. Soc. 126 (2004) 2355–2361.

[19] N. Nishiyama, Arnida, W.-D. Jang, K. Date, K. Miyata, K. Kataoka, Photochemical enhancement of transgene expression by polymeric micelles incorporating plasmid DNA and dendrimer-based photosensitizer, J. Drug Target 14 (2006) 413–424.

[20] N. Kanayama, N. Nishiyama, S. Fukushima, K. Itaka, W.-D. Jang, K. Miyata, Y. Yamasaki, K. Kataoka, PEG-based biocompatible block catiomer with high-buffering capacity for the construction of polyplex micelles showing efficient gene transfer toward primary cells, ChemMedChem 1 (2006) 439–444.

[21] A.C.H. Ng, X. Li, D.K.P. Ng, Synthesis and photophysical properties of non-aggregated phthalocyanines bearing dendritic substitutes, Macromolecules 32 (1999) 5292–5298.

[22] W.-D. Jang, Y. Nakagishi, N. Nishiyama, S. Kawauchi, Y. Morimoto, M. Kikuchi, K. Kataoka, Polyion complex micelle for photodynamic therapy: incorporation of dendritic photosensitizer excitable at long wavelength with enhanced cellular uptake, J. Control. Rel. 113 (2006) 73–79.

[23] H. Niwa, K. Yamamura, J. Miyazaki, Efficient selection for high-expression transfectants with a novel eukaryotic vector, Gene 108 (1991) 193–199.

[24] A. Harada, K. Kataoka, Formation of polyion polyplex micelles in aqueous milieu from a pair of oppositely-charged block copolymers with poly (ethylene glycol) segment, Macromolecules 285 (1995) 294–5299.

[25] M.B. Hansen, S.E. Nielsen, K. Berg, Re-examination and further development of a precise and rapid dye method for measuring cell growth/cell kill, J. Immunol. Methods 119 (1989) 203–210.

[26] K. Itaka, A. Harada, K. Nakamura, H. Kawaguchi, K. Kataoka, Evaluation by fluorescence resonance energy transfer of the stability of non viral gene delivery vectors under physiological conditions, Biomacromolecules 3 (2002) 841–845.

[27] J.S. Zhang, F. Liu, L. Huang, Implication of pharmacokinetic behavior of lipoplex for its inflammatory cytotoxicity, Adv. Drug Deliv. Rev. 57 (2005) 689–698.

[28] R.K. Jain, D. Fukumura, D.E.J.G.J. Dolmans, Photodynamic therapy for cancer, Nat. Rev., Cancer 3 (2003) 380–387.

[29] Y. Bae, N. Nishiyama, S. Fukushima, H. Koyama, Y. Matsumura, K. Kataoka, Preparation and biological characterization of polymeric micelle drug carriers with intracellular pH-triggered drug release property: tumor permeability, controlled subcellular drug distribution, and enhanced *in vivo* antitumor efficacy, Bioconjug. Chem. 16 (2005) 122–130.

[30] N. Nishiyama, S. Okazaki, H. Cabral, M. Miyamoto, Y. Kato, Y. Sugiyama, K. Nishio, Y. Matsumura, K. Kataoka, Novel cisplatin-incorporated polymeric micelles can eradicate solid tumors in mice, Cancer Res. 63 (2003) 8977–8983.

[31] J. Moan, K. Berg, A. Anholt, K. Madslien, Sulfonated aluminum phthalocyanines as sensitizers for photochemotherapy. Effects of small doses on localization, dye fluorescence and photosensitivity in V79 cells, Int. J. Cancer 58 (1994) 865–870.

Journal of Drug Targeting, July 2006; 14(6): 413–424

informa
healthcare

Photochemical enhancement of transgene expression by polymeric micelles incorporating plasmid DNA and dendrimer-based photosensitizer

NOBUHIRO NISHIYAMA[1], ARNIDA[2], WOO-DONG JANG[2], KOTOE DATE[2], KANJIRO MIYATA[2], & KAZUNORI KATAOKA[1,2,3,4]

[1]*Center for Disease Biology and Integrative Medicine, Graduate School of Medicine, The University of Tokyo, 7-3-1 Hongo, Bunkyo-ku, Tokyo 113-0033, Japan,* [2]*Department of Materials Engineering, Graduate School of Engineering, The University of Tokyo, 7-3-1 Hongo, Bunkyo-ku, Tokyo 113-8656, Japan,* [3]*Core Research Program for Evolutional Science and Technology (CREST), Japan Science and Technology Agency (JST), Tokyo, Japan, and* [4]*Center for NanoBio Integration, The University of Tokyo, 7-3-1 Hongo, Bunkyo-ku, Tokyo 113-8656, Japan*

(Received 15 November 2005; revised 19 January 2006; in final form 2 February 2006)

Abstract

The development of synthetic gene carriers has recently received much attention; however, they might lack the ability to control the transgene expression. The use of external stimuli for enhancement of the transgene expression may be a promising approach for the site-directed transfection *in vivo*. In this regard, a new technology of "photochemical internalization (PCI)" has recently been reported, in which the endosomal escape of gene carriers is assisted by photodamage of the endosomal membrane with co-incubating photosensitizers. To apply this technology for systemic gene delivery, the development of appropriate carrier systems for both the plasmid DNA (pDNA) and photosensitizer is of crucial importance. Also, the photocytotoxicity accompanied by the photochemical enhancement of the gene expression may need to be reduced. In this study, the combinational formulation of polymeric micelles incorporating pDNA and a dendrimer-based photosensitizer (DP) (dendrimer phthalocyanine (DPc)) was applied in the PCI-mediated transfection *in vitro* and then, estimating its potential utility for *in vivo* applications. The PCI using the polymeric micelle system achieved a remarkable photochemical enhancement of the transgene expression while maintaining an approximate 80% cell viability over a wide range of the DPc concentrations and light doses. Thus, this system may be promising for *in vivo* PCI-mediated gene delivery.

Keywords: *Gene therapy, non-viral gene carriers, polymeric micelles, photochemical internalization (PCI), dendrimer*

Introduction

Recently, non-viral gene carriers based on cationic lipids and synthetic polymers have received much attention as an attractive alternative to viral vectors in gene therapy (Merdan et al. 2002; Ogris and Wagner 2002; Pack et al. 2005). In addition to several advantages, such as safety, simplicity of use and ease of mass production, the variety of chemical designs of the constituent lipids and polymers is a strong motivation to develop novel gene carriers. In particular, considerable efforts have been devoted to the development of biocompatible gene carriers, which might show longevity during blood circulation and effectively accumulate at the target site (Ogris and Wagner 2002; Pack et al. 2005). In this regard, a promising approach is the use of poly(ethylene glycol) (PEG)–polycation block copolymers, since they spontaneously associate with plasmid DNA (pDNA) to form the nano-scaled polyplex micelles, in which the pDNA/polycation polyplex core is surrounded by a dense and hydrophilic PEG palisade (Katayose and Kataoka 1997; Harada-Shiba et al. 2002; Itaka et al. 2003; Miyata et al. 2004; Wakebayashi et al. 2004; Fukushima et al. 2005). Indeed, the polyplex micelles formed between pDNA and PEG–poly(L-lysine)

Correspondence: K. Kataoka, Department of Materials Engineering, Graduate School of Engineering, The University of Tokyo, 7-3-1 Hongo, Bunkyo-ku, Tokyo 113-8656, Japan. E-mail: kataoka@bmw.t.u-tokyo.ac.jp

ISSN 1061-186X print/ISSN 1029-2330 online
DOI: 10.1080/10611860600834508

(A)

CH_3-$(OCH_2CH_2)_m$-CH_2-NH-(CO-CH-NH)$_n$-H
$(CH_2)_4$
$NH_3^+Br^-$

(B)

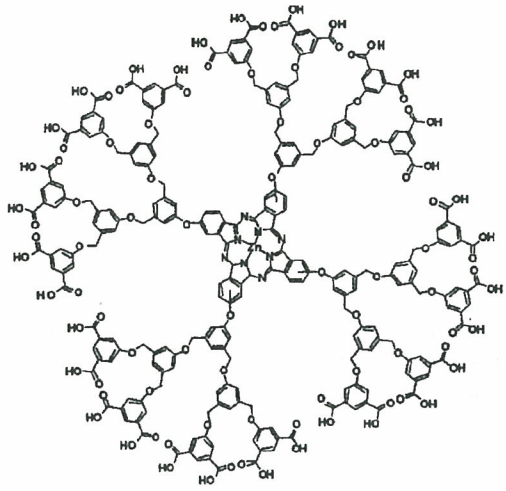

Figure 1. Chemical structures of PEG–PLL block copolymer (A) and DPc (B).

(PEG–PLL) block copolymers (Figure 1(A)) showed an improved stability in proteinous media (Itaka et al. 2003) and prolonged blood circulation in mice (Harada-Shiba et al. 2002). However, the limited transfection ability of the pDNA/PEG–PLL polyplex micelle is a major issue in their applications for *in vivo* gene therapy (Harada-Shiba et al. 2002; Itaka et al. 2003; Miyata et al. 2004). It has been suggested that such a low gene transferring ability of the polyplex micelles might be due to their inefficient transport from the endosome/lysosome to the cytoplasm (Itaka et al. 2003; Miyata et al. 2004).

Other than a high transfection efficiency, site-specific gene transfer has been strongly desired for gene vectors to ensure the safety and effectiveness for *in vivo* gene therapy. However, the existing vectors including viral and non-viral ones still have the problem of non-specific gene transfection. Recently, a smart approach called "photochemical internalization (PCI)" was introduced by Høgset and Berg et al. to overcome both the limited transfection efficiency and the lack of specificity of non-viral gene vectors. The PCI using hydrophilic photosensitizers allows the photochemical disruption of the endosomal/lysosomal membranes, facilitating the cytoplasmic delivery of macromolecular compounds such as genes and proteins (Berg et al. 1999; Høgset et al. 2000, 2002, 2004; Prasmickaite et al. 2001). This approach indeed achieved an appreciable increase in the transfection efficiency upon light illumination under *in vitro* conditions; however, it was accompanied by the problem of photocytotoxicity (Høgset et al. 2000). It should be noted that the photocytotoxicity might not be directly correlated with the photodamage to the endosomal/lysosomal membranes, but the photodamaging of other susceptible organelles may account for the cytotoxicity involved in the PCI (Macdonald and Dougherty 2001; Moan et al. 1994). Hence, the spatially localized photodamage limited to the endosome/lysosome is assumed to lead to the enhanced photochemical transfection with reduced cytotoxicity (Nishiyama et al. 2005). Also, in addition to controlled localization in the intracellular compartment, photosensitizers might need to be systemically delivered to the target tissue to achieve a successful PCI-mediated gene delivery *in vivo*.

In this study, the PCI using polymeric micelles incorporating DPs (dendrimer phthalocyanine (DPc) illustrated in Figure 1(B)) was carried out to enhance the gene transferring ability of the aforementioned pDNA/PEG–PLL polyplex micelle in a light-selective manner (Figure 2). DPc possesses a center phthalocyanine molecule surrounded by a second generation of aryl ether dendrons and 32 carboxyl groups on the periphery of the DPc allow the formation of polyion complex (PIC) micelles through an electrostatic interaction with the PEG–PLL block copolymers

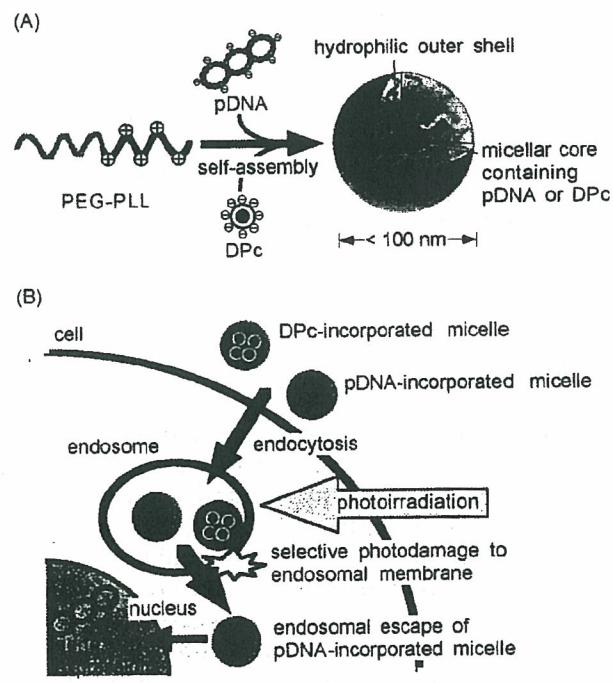

Figure 2. (A) Formation of polymeric micelles through the electrostatic interaction between PEG–PLL and pDNA or DPc. (B) Scheme for itinerary of the pDNA- and DPc-incorporated micelles in the PCI-mediated transfection. Both polymeric micelles are assumed to be taken up by the cell through the endocytic pathway and the localization of the DPc-incorporated micelles in the endosome may allow the selective photodamaging of the endosomal membrane upon photoirradiation, thereby inducing the cytoplasmic delivery of the pDNA-incorporated micelles.

(Stapert et al. 2000; Ideta et al. 2005; Jang et al. 2005). In this strategy, both the pDNA- and DPc-incorporated polymeric micelles are expected to exhibit prolonged blood circulation after intravenous administration and selectively accumulate in the target tissues such as solid tumors as previously reported (Kwon et al. 1994; Nishiyama et al. 2003a,b; Bae et al. 2005). Also, both micelles are assumed to show the same subcellular localization at the target site due to similar particle sizes and surface properties. The control of the localization of the photosensitizers and gene carriers at both the tissue and subcellular levels appears to be a prerequisite for the PCI-mediated gene delivery *in vivo*. Furthermore, the DPc-incorporated micelles may cause highly selective photodamage to the endosomal/lysosomal membranes, because polymeric micelles are assumed to be taken up by the cell through the endocytic pathway (Figure 2(B)). Thus, the combinational use of the pDNA- and DPc-incorporated micelles may be a promising approach to the PCI-mediated gene delivery. In the present study, the feasibility of our strategy was confirmed by the enhanced *in vitro* transfection with limited cytotoxicity under different conditions, thus featuring the possibilities for future *in vivo* applications.

Materials and methods

Materials

N^{ε}-Z-L-Lysine and bis(trichloromethyl) carbonate (triphosgene), for the synthesis of PEG–PLL, were purchased from Sigma-Aldrich Co., Inc. (St Louis, MO) and Tokyo Kasei Co., Ltd (Tokyo, Japan), respectively. α-Methoxy-ω-amino-poly(ethylene glycol) (MeO–PEG–NH_2, MW = 12 kg/mol) was purchased from Nippon Oil and Fats, Co., Ltd. Chemicals for the dendrimer synthesis were purchased from Tokyo Kasei and Sigma-Aldrich. *n*-Pentanol and 1,8-diazabicyclo-(5,4,0)-undec-7-ene (DBU) were purchased from Tokyo Kasei and used without further purification. All solvents for the polymer syntheses were distilled just before use.

A pDNA, pCAcc + Luc, containing a firefly luciferase cDNA driven by a CAG promoter (Niwa et al. 1991) was provided by the RIKEN Bioresource Center (Tsukuba, Japan). pDNA was amplified in competent DH5α *Escherichia coli* and purified by a HiSpeed Plasmid Maxi Kit from Qiagen Co., Inc. (Valencia, CA). Sulfonated aluminum phthalocyanine ($AlPcS_{2a}$) (aluminum phthalocyanine with two sulfonate groups on adjacent phthalate rings) was purchased from Frontier Scientific Co., Inc. (Logan, UT).

Polymer synthesis and characterization

The synthesis of the ionic DPc was performed according to the method reported by Ng's group (Ng et al. 1999). The second generation of dendritic phenol was reacted with 4-nitrophthalonitrile by an alkali-mediated coupling reaction to obtain the corresponding dendritic phthalonitrile, which was then treated with $Zn(OAc)_2$ and DBU in *n*-pentanol to give DPc. The obtained DPc was treated with a THF/H_2O mixture solution containing NaOH to obtain the ionic DPc (MW: 4904). The absorption spectra in an aqueous solution revealed that DPc exhibits a B band absorption at 350 nm and a strong Q band absorption at 685 nm, indicating a monomeric dispersion without agglomerization.

PEG–PLL block copolymers (PEG: MW = 12 kg/mol) having different polymerization degrees of the PLL segment (49 and 73; the code names are 12–49 and 12–73, respectively) were synthesized as previously reported (Harada and Kataoka 1995). Briefly, the *N*-carboxy anhydride of N^{ε}-Z-L-lysine was polymerized from the ω-NH_2 group of CH_3O–PEG–NH_2 in DMF under Ar to obtain PEG–PLL(Z), followed by deprotection of the Z group. The polymerization degree of the PLL segments and the narrowly distributed nature of the synthesized PEG–PLL(Z) were determined by the ^{1}H-NMR and the gel permeation chromatography (GPC), respectively.

Preparation of DPc-incorporated micelles

The DPc-incorporated micelles were prepared by mixing DPc and PEG–PLL 12–49 at a stoichiometric charge ratio. In a typical procedure, PEG–PLL was dissolved in a 10 mM NaH_2PO_4 solution (0.457 ml) and added to DPc in a 10 mM Na_2HPO_4 solution (1.0 ml) to give the solution containing the DPc-incorporated micelles in a 10 mM phosphate buffered solution (pH 7.4). The size and size distribution (polydispersity index) of the micelles were measured by dynamic light scattering (DLS) measurements using a DLS-7000 instrument with a vertically polarized incident beam of 488 nm wavelength from an Ar ion laser (Otsuka Electronics Co., Ltd, Osaka, Japan).

Preparation of pDNA/PEG–PLL polyplex micelles

pDNA and PEG–PLL 12–73 were separately dissolved in a 10 mM Tris–HCl buffer (pH 7.4). The PEG–PLL solution with varying concentrations was then added to the pDNA solution to form the polyplex micelles with different N/P ratios, which denote the ratio of the molar concentration of the cationic amino groups in PEG–PLL to that of the phosphate groups in DNA. The polyplex micelle solution was maintained overnight at ambient temperature before use.

The size and size distribution of the polyplex micelles were measured by the DLS measurement using the DLS-7000. The effect of the N/P ratios on the pDNA condensation in the polyplex micelles was estimated from a decrease in the fluorescence intensity

of ethidium bromide (EtBr) due to the exclusion from the DNA double strand. The polyplex micelle solutions at various N/P ratios were adjusted to 20 μg pDNA/ml with 0.4 μg EtBr/ml by adding 10 mM Tris–HCl buffer containing EtBr. The ratio of the residual molar concentration of EtBr to that of the base pair in pDNA was 0.033. The fluorescence measurements (Ex: 510 nm; Em: 590 nm) were carried out at 25°C using a FP-777 spectrofluorometer from Jasco Co., Ltd (Tokyo, Japan). The results were expressed as the relative fluorescence intensity to the intensity of the free pDNA solution with EtBr.

In vitro *transfection and cytotoxicity assays*

Human cervical carcinoma HeLa cells or human hepatoma HuH-7 cells (10,000 cells) were seeded and cultured on a 24-well culture plate (BD Bioscience, Franklin Lakes, NJ) for 24 h prior to the transfection (cell seeding density: 1400 cells/cm^2). The pDNA/-PEG–PLL polyplex micelle solution prepared at a defined N/P ratio containing 1 μg pDNA and the photosensitizer solutions (i.e. $AlPcS_{2a}$, DPc and DPc-incorporated micelle) with various concentrations were added to the cells in 0.5 ml of Dulbecco's modified Eagle's medium (DMEM) containing 10% fetal bovine serum (FBS), followed by a 6 or 24 h incubation and medium replacement with a fresh one. The culture plates were photoirradiated using a 300 W halogen lamp (fluence rate: 3.0 mW/cm^2) equipped with a band-pass filter (400–700 nm) with increased fluence (2.7–8.1 J/cm^2). After a 48 h post-incubation, the transfection efficiency and cell viability were examined. In the transfection assay, the cells were lysed and the luciferase activity of the lysate was measured using the Luciferase Assay System (Promega, Madison, WI) and a Lumat LB9507 luminometer (Berthold Technologies, Bad Wildbad, Germany). The results are expressed as light units per milligram of cell protein determined by a BCA assay kit (Pierce, Rockford, IL). On the other hand, the cell viability was evaluated by the 3-(4,5-dimethylthiazol-2-yl)-2,5-diphenyltetrazolium bromide (MTT) (Dojindo Laboratories, Kumamoto, Japan) assay.

Results and discussion

In this study, we investigated the feasibility of using polymeric micelles as a nanocarrier for the pDNA and photosensitizer in the PCI-mediated gene delivery *in vitro*. As previously described, a simple mixing of pDNA and PEG–PLL results in the formation of the polyplex micelles (Katayose and Kataoka 1997; Itaka et al. 2003). The size and polydispersity indices of the mixtures prepared at various N/P ratios are shown in Figure 3(A) and (B), indicating the formation of the polyplex micelles with sizes of 90–140 nm and a moderate polydispersity over a broad range of N/P ratios (0.5–6). The histogram analysis in the DLS measurement revealed that the polyplex micelles possess a unimodal size distribution (data not shown). Figure 3(C) shows the effect of the N/P ratios

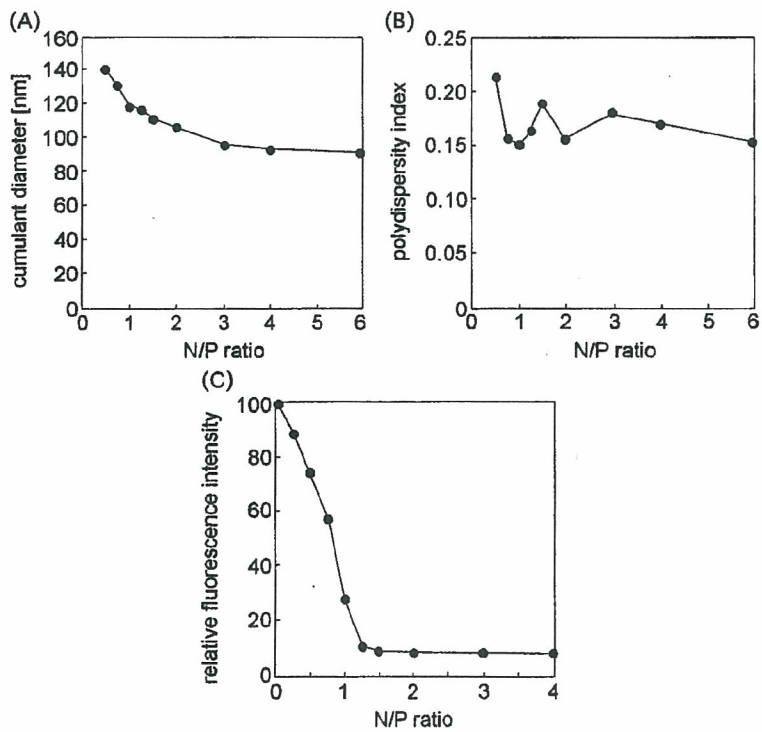

Figure 3. Changes in the cumulant diameter (A), the polydispersity index (μ_2/Γ^2) (B) and the fluorescence intensity of EtBr (C) for the pDNA/PEG–PLL polyplex micelles prepared at different N/P ratios.

on the exclusion of EtBr from the pDNA/PEG–PLL complexes. Apparently, the fluorescence intensity of EtBr leveled off above the N/P ratio of 1.2, suggesting this to be a minimum N/P ratio to fully condense pDNA. On the other hand, it is generally difficult to incorporate conventional photosensitizers into nanocarriers, because they have a hydrophobic structure with a large π-conjugation domain that easily forms aggregates. Recently, we reported DPs as a promising photosensitizer applicable for drug delivery (Nishiyama et al. 2003a,b). DPs have a focal sensitizer core segregated by a 3D dendritic architecture, which might allow effective photochemical reactions even at a high concentration and the periphery with tailored functional groups. Ionic DPs with cationic or anionic peripheral groups show a good solubility in aqueous media and form a PIC micelle with oppositely charged block copolymers (Stapert et al. 2000). We have demonstrated that polymeric micelles incorporating DPs are promising photosensitizer formulations for photodynamic therapy (Ideta et al. 2005; Jang et al. 2005). In the present study, the DPc-incorporated micelles were spontaneously formed through an electrostatic interaction between DPc and PEG–PLL. The DLS measurement revealed that the DPc-incorporated micelles had a diameter of 50 nm with a narrow size distribution (unimodal, polydispersity index (μ_2/Γ^2): 0.12). The DPc-incorporated micelles have strong Q-band absorptions at 630 and 685 nm for excitation of the DPc, thus, expecting a deeper tissue penetration of light for *in vivo* applications.

This study's objective is to investigate the feasibility of the PCI-mediated gene delivery using polymeric micelles as nanocarriers for pDNA and DPc. First, the optimal N/P ratio of the pDNA/PEG–PLL polyplex micelles on the photochemical transfection was determined. Figure 4(A) and (B) show the photochemical enhancement of the transfection of the pDNA/PEG–PLL polyplex micelles prepared at the N/P ratio of 1.2 or 2.0 and the concomitant photocytotoxicity, respectively. In this experiment, HeLa cells were photoirradiated at the fluence of 5.4 J/cm^2 after a 6 h incubation with the combination of the pDNA- and DPc-incorporated micelles and medium replacement with a fresh one, followed by a 48 h post-incubation. The polyplex micelles prepared at N/P = 1.2 achieved more than a 100-fold photochemical enhancement of the gene expression with 20–25% decreases in cell viability, whereas those prepared at N/P = 2.0 showed only a 10–30-fold gene expression enhancement with comparable decreases in cell viability. Thus, the polyplex micelles prepared at N/P = 1.2 might be more efficient in the PCI-mediated transfection compared with those prepared at N/P = 2.0. It should be noted that naked plasmid did not show any detectable gene transfection, regardless of the utilization of the PCI (data not shown), suggesting the necessity of appropriate gene

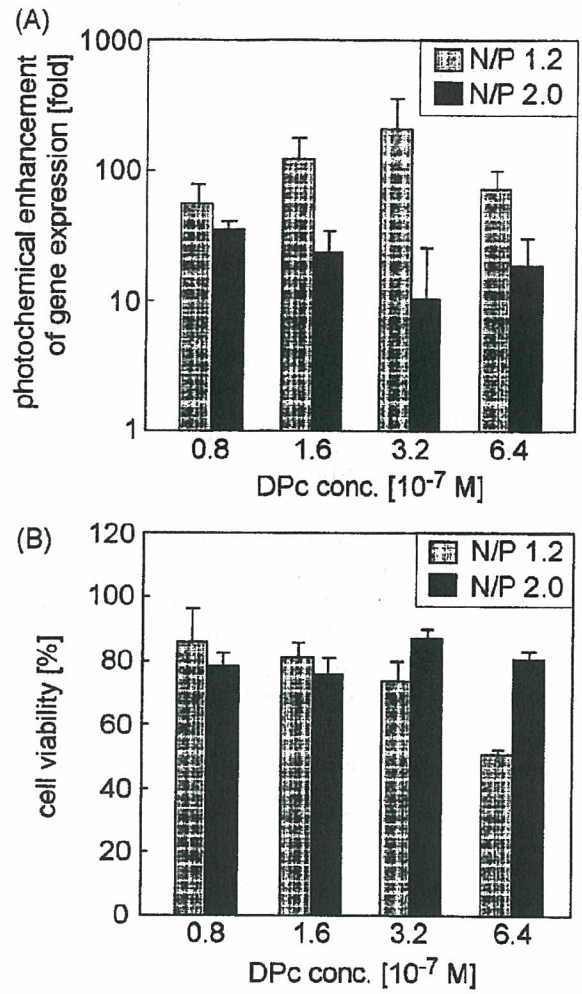

Figure 4. The effect of the N/P ratio of the polyplex micelles on the photochemical enhancement of the gene expression (A) and photocytotoxicity (B) in the PCI-mediated transfection using DPc-incorporated micelle. The light irradiation (fluence: 5.4 J/cm^2) was performed 6 h after incubation with the pDNA- and DPc-incorporated micelles, followed by 48 h post-incubation in a fresh medium.

carriers for the PCI-mediated gene delivery. Interestingly, the polyplex micelles prepared at the N/P ratios of 1.2 and 2.0 showed similar transfection efficiencies in the absence of a photosensitizer and light (5,08,000 ± 1,49,000 vs. 4,17,000 ± 1,69,000 RLU/mg protein (mean ± SD)). These results suggest that an excess of PEG PLL might decrease the efficacy of the photochemical transfection. In the PCI-mediated transfection, the efficient cytoplasmic delivery of the polyplex micelles can be achieved by photochemical rupture of the endosomal membrane; therefore, the release of pDNA from the polyplex micelles in the cytoplasm or nuclei may be a rate-limiting process in the gene transfection. The polyplex micelles at N/P = 1.2 are expected to show more efficient pDNA release than those at N/P = 2.0, thereby showing a higher photochemical enhancement of the transfection. Based on these results,

polyplex micelles prepared at N/P = 1.2 were used for further investigations.

The transfection efficiency and cytotoxicity of the polyplex micelles co-incubated with the DPc-incorporated micelles in the presence or absence of light irradiation (fluence: 5.4 J/cm^2) are shown in Figure 5(A) and (B), respectively. The same experimental procedures as in Figure 4 were applied in this study. Based on these results, the PCI using the DPc-incorporated micelles achieved a 56–212-fold photochemical enhancement of the transfection of the polyplex micelles while maintaining an approximately 80% cell viability over a wide range of DPc concentrations (0.4×10^{-7}–3.2×10^{-7} M) and showed an approximately 50% decrease in viability above the critical DPc concentration (6.4×10^{-7} M). Note that a similar photochemical enhancement of the transfection was observed when 293 T cells were used (data not shown). The maximal transfection level achieved by the PCI using the DPc-incorporated micelles was comparable to that obtained using hydroxychloroquine (hc), which has been demonstrated to be a potent endosomotropic agent (Itaka et al. 2004) (Figure 5(A)). Interestingly, the transfection efficiency of the polyplex micelles decreased as the concentration of the DPc-incorporated micelles increased, particularly under non-irradiated conditions (Figures 5(A) and 6(A)), thus leading to a remarkably high light-selectivity of the gene transfection. Such a DPc concentration-dependent decrease in the transfection efficiency of the polyplex micelles was not observed in the PCI using DPc alone (Figure 7(A)). There may be two possible explanations for this observation. First, the polyplex micelles may compete with the DPc-incorporated micelles in the cellular uptake due to similar particle sizes and surface properties. In Figure 5(A), the molar concentration of the DPc-incorporated micelles was estimated to be comparable to or 20-fold higher than that of the polyplex micelles at the DPc concentration of 2.0×10^{-8} or 6.4×10^{-7} M, respectively. An increase in the DPc concentration decreases the molar ratio of the pDNA-incorporated micelles to the DPc-incorporated micelles in the medium, leading to a decreased cellular uptake of the pDNA-incorporated micelles. Alternatively, the pDNA- and DPc-incorporated micelles may interact each other, thereby decreasing the transfection efficiency. Indeed, we observed in Figure 4(A) that an excess of PEG–PLL could decrease the transfection efficiency of the polyplex micelles in the PCI-mediated transfcetion. These possibilities may also account for the DPc concentration-dependent decrease in the transfection efficiency.

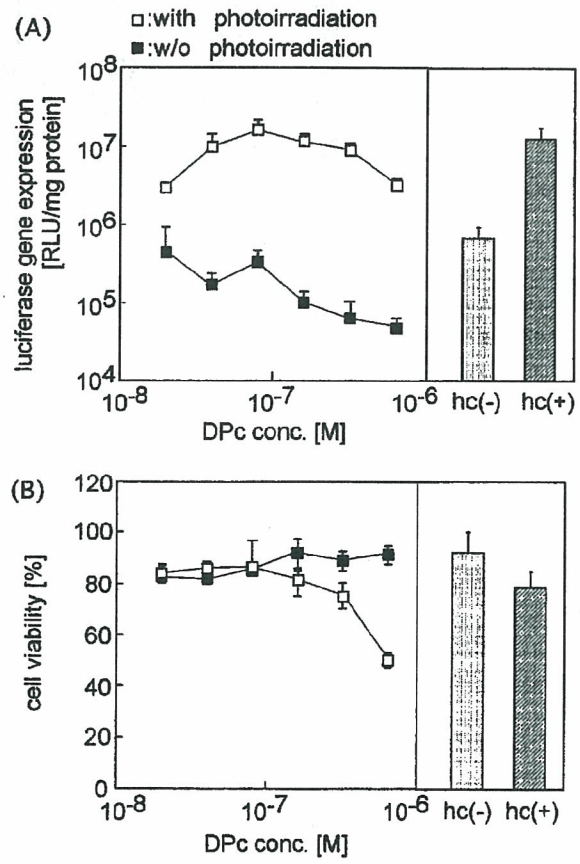

Figure 5. The effect of the DPc concentration on the transfection efficiency (A) and photocytotoxicity (B) in the PCI-mediated transfection using the DPc-incorporated micelles. The light irradiation (fluence: 5.4 J/cm^2) was performed 6 h after incubation with the pDNA- and DPc-incorporated micelles, followed by 48 h post-incubation in a fresh medium.

Regarding changes in cell viability in Figure 5(B), a DPc concentration-dependent decrease in cell viability was observed at the DPc concentrations above 1.6×10^{-7} M, while a DPc concentration-independent 10–20% decrease in cell viability was observed below 1.6×10^{-7} M DPc, regardless of photoirradiation. It is assumed that the DPc concentration-dependent decrease in cell viability observed at the region of high-DPc concentration might be attributable to the photochemical reactions in the PCI-mediated transfection. On the other hand, the 10–20% decrease in cell viability at the lower DPc concentration even without photoirradiation may be inducible by the DPc-incorporated micelles, since the pDNA-incorporated micelles alone did not show an appreciable cytotoxicity (Figures 6(C) and 7(C)). Nevertheless, such a 10–20% decrease in cell viability, of which the mechanisms remain to be clarified yet, is still in a tolerable range and is unlikely to be the serious limitations of this strategy.

The effects of the DPc concentration and fluence on the transfection efficiency of the polyplex micelles, photochemical enhancement of the transfection and photocytotoxicity in the PCI using the DPc-incorporated micelles were completely examined and the results are shown in Figure 6(A)–(C), respectively. Similarly, the PCI-mediated transfection of the pDNA/PEG–PLL polyplex micelles was carried out

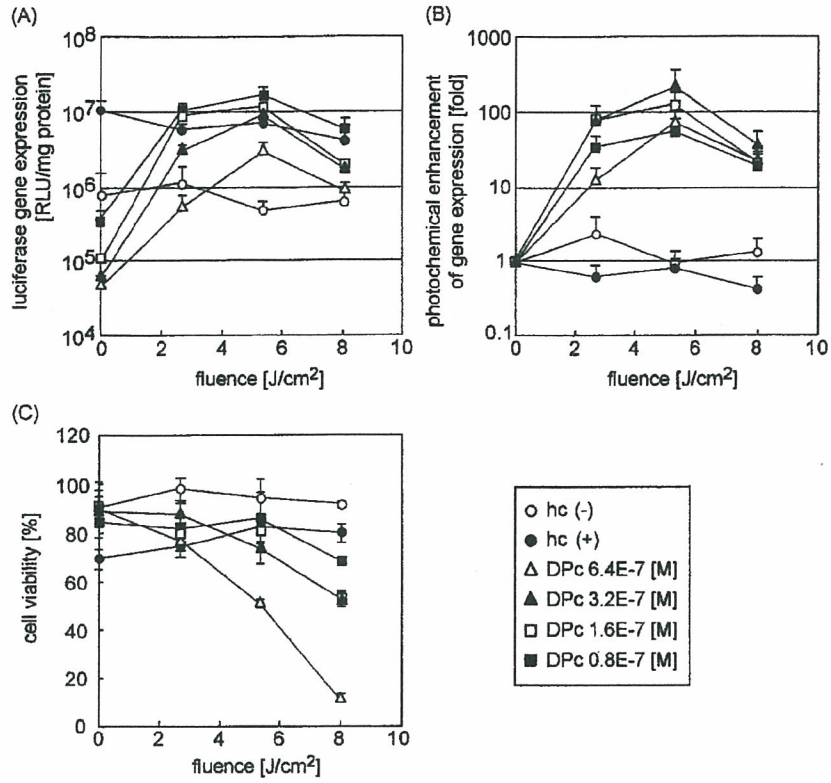

Figure 6. The effects on the DPc concentration and fluence on the transfection efficiency (A), photochemical enhancement of the gene expression (B) and photocytotoxicity (C) in the PCI-mediated transfection using the DPc-incorporated micelles. The light irradiation was performed 6 h after incubation with the pDNA- and DPc-incorporated micelles, followed by 48 h post-incubation in a fresh medium. The "hc" strands for hydroxychloroquine.

using DPc alone or $AlPcS_{2a}$, which was demonstrated to be an effective photosensitizer in the PCI (Høgset et al. 2002, 2004). These results are shown in Figures 7 and 8, respectively. Also, to easily compare the main differences between the results in Figures 6–8, the effects of each photosensitizer on the photochemical enhancement of the gene expression and cell viability at the fluence of 5.4 J/cm^2 are summarized in Table I. In the PCI using DPc alone, the highest transfection efficiency of the polyplex micelles was obtained with a 25–50% reduced cell viability (Figure 7(A) and (C)). The PCI using $AlPcS_{2a}$ showed a transfection activity comparable to that using the DPc-incorporated micelles; however, the photochemical enhancement of the transgene expression was accompanied by an inevitable photocytotoxicity (Figure 8(A) and (C)). Eventually, the PCI using the combination of the pDNA- and DPc-incorporated micelles showed the highest photochemical enhancement of the gene transfection of the polyplex micelles (Figure 6(B)), which may be attributed to the reduced transfection efficiency at comparatively high-concentrations of the DPc-incorporated micelles under non-irradiated conditions as discussed above as well as actual increases in the transfection efficiency. Such a high-light-selectivity of the gene transfection might be advantageous for accomplishing the site-directed gene transfer using the PCI concept. More importantly, the PCI using the DPc-incorporated micelles showed an appreciably wide range of safe DPc concentrations and light doses, in which a remarkable enhancement of the transfection was achieved without a substantial decrease in the cell viability (Figure 6(B) and (C)). The efficacy of this system was prominent even when compared with those of other systems using DPc alone and $AlPcS_{2a}$ as shown in Table I.

To achieve a systemic PCI-mediated gene delivery utilizing micellar nanocarriers, polymeric micelles are required to accumulate in the target tissues and be taken up by the target cells, of which processes are known to occur in a time-dependent manner. On the other hand, the timing of the photoirradiation may be a critical factor in the PCI-mediated transfection (Prasmickaite et al. 2001). Hence, the effect of the photoirradiation timing on the photochemical transfection was then investigated. First, the effect of the prolonged incubation before photoirradiation was examined: after a 24 h continuous incubation with the combination of the pDNA- and DPc-incorporated micelles, HeLa cells were subjected to the medium replacement, followed by photoirradiation at the fluence of 5.4 J/cm^2. The transfection efficacy was evaluated after a further 48 h of post-incubation. As seen in Figure 9, an approximately 50-fold photochemical enhancement in the gene expression while

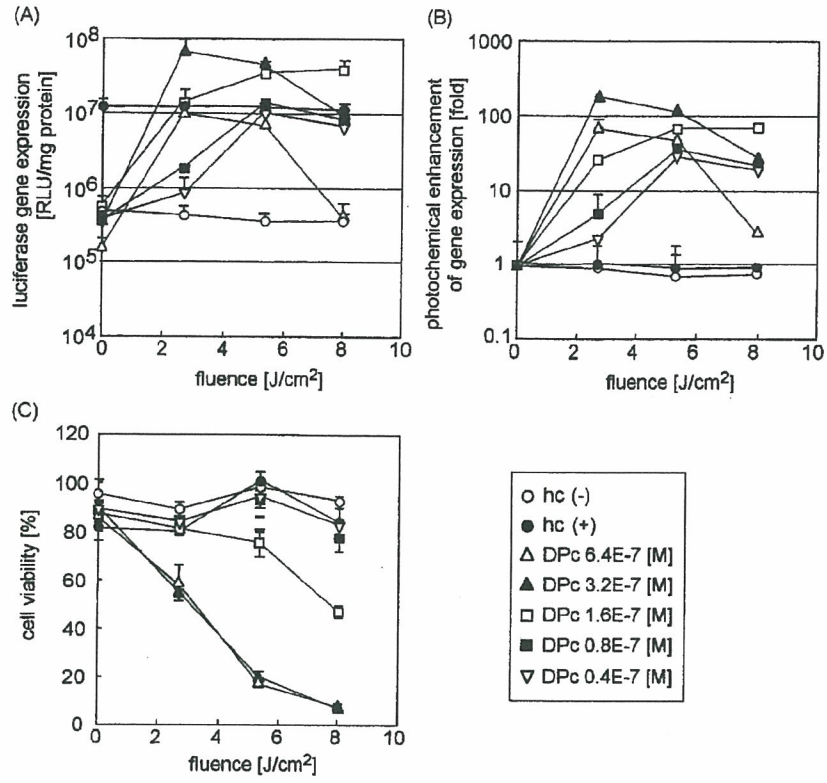

Figure 7. The effects on the DPc concentration and fluence on the transfection efficiency (A), photochemical enhancement of the gene expression (B) and photocytotoxicity (C) in the PCI-mediated transfection using DPc alone. The light irradiation was performed 6 h after incubation with the pDNA-incorporated micelles and free DPc, followed by 48 h post-incubation in a fresh medium.

maintaining more than an 80% cell viability was obtained under this condition, which appears to be consistent with Figure 5. Thus, the PCI using the DPc-incorporated micelles might be effective even after a prolonged incubation before photoirradiation. Note that the transfection efficiencies of the polyplex micelles under both irradiated and non-irradiated conditions decreased as the DPc concentration increased (Figure 9(A)), which may be due to the decreased cellular uptake of the polyplex micelles and/or interaction between the pDNA- and DPc-incorporated micelles as discussed above. In a second set of experiments, a certain lag time was placed before the photoirradiation of the HeLa cells in freshly replaced medium after a 6 h incubation with the combinational formulation of pDNA- and DPc-incorporated micelles. The transfection efficacy was evaluated 48 h after the photoirradiation (5.4 J/cm^2). As shown in Figure 10, post-incubation in the micelle-free medium after the 6 h treatment with the combinational micellar formulation resulted in a time-dependent decrease in the efficacy of the PCI-mediated transfection. This result seems to be consistent with the previous observation by Prasmickaite et al. (2001) suggesting that, in the PCI-mediated transfection, gene carriers may need to be translocated into the cytosol before their movement from the endosome to the lysosome. Therefore, to achieve a successful *in vivo* PCI-mediated gene delivery, the timing of the photoirradiation should be optimized in consideration of the balance between the effective accumulation of gene carriers as well as photosensitizers in the target cells and the prompt photo-induced translocation of gene carriers from the endosome to the cytosol before their movement to the lysosome.

The PCI is a smart concept, which can be basically used for the site-directed transfection in a light-inducible manner. In previous studies, AlPcS$_{2a}$ was demonstrated to be effective in the PCI (Høgset et al. 2002, 2004); however, the photochemical enhancement of the transfection was accompanied by the photocytotoxicity (Høgset et al. 2000). Although AlPcS$_{2a}$ is known to be internalized by the endocytic pathway, it is likely that AlPcS$_{2a}$ may interact with the plasma membrane to some extent as well as relocalize to some cytoplasmic organelles such as the mitochondria and endoplasmic reticulum during the photoirradiation, thereby inducing the inevitable photocytotoxicity (Moan et al. 1994; Macdonald and Dougherty 2001). Hence, considerable efforts have been devoted to the optimization of the experimental conditions for reducing the photocytotoxicity in the PCI-mediated transfection (Høgset et al. 2000). Also, the delivery of photosensitizers to the target cell should be taken into consideration in order to accomplish the *in vivo* PCI-mediated gene delivery.

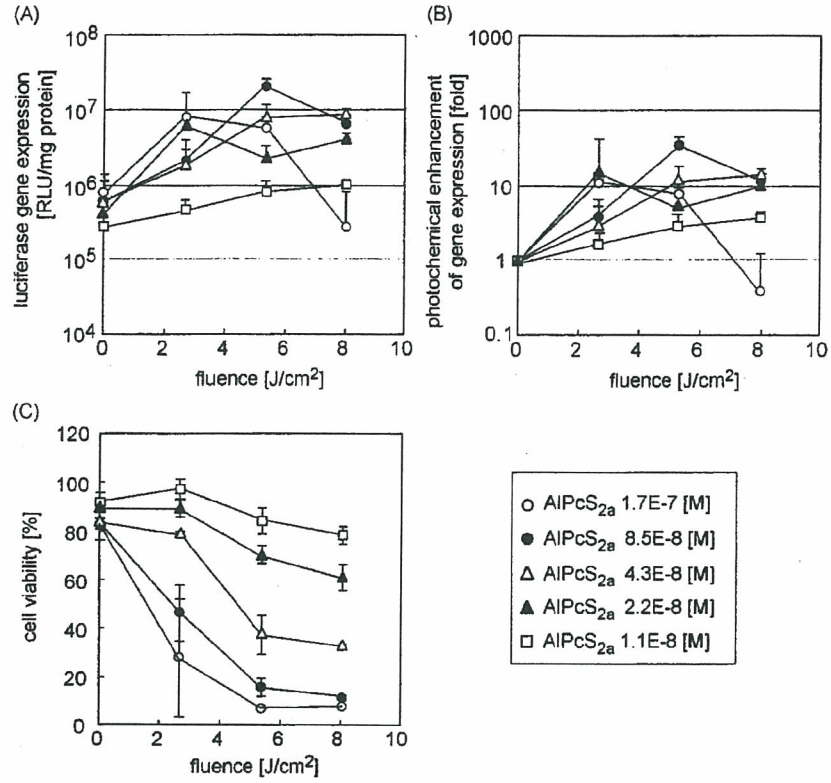

Figure 8. The effects on the $AlPcS_{2a}$ concentration and fluence on the transfection efficiency (A), photochemical enhancement of the gene expression (B) and photocytotoxicity (C) in the PCI-mediated transfection using $AlPcS_{2a}$. The light irradiation was performed 6 h after incubation with the pDNA-incorporated micelles and $AlPcS_{2a}$, followed by 48 h post-incubation in a fresh medium.

In this regard, we have recently developed DPc as a new photosensitizer for the PCI (Nishiyama et al. 2005). It has been demonstrated that the anionic DPc might electrostatically interact with the surface of the cationic polyplex to form the ternary complex enveloped with DPc, thus giving the same internalization and subcellular localization between DPc and the polyplex. Meanwhile, DPc exhibited a pH-dependent membrane binding ability, allowing the selective photodamaging of the endosomal membrane. Consequently, the ternary complex showed more than 100-fold photochemical enhancement of the gene expression with reduced photocytotoxicity on the cultured cells and *in vivo* light-selective gene transfer to the conjunctival tissues in rat eyes (Nishiyama et al. 2005). Thus, it was suggested that the design of the ternary complex might be effective for the PCI-mediated gene delivery; however, the ternary complex system is unlikely to be used for the systemic delivery. It is known that highly negatively-charged macromolecules can be excluded from the blood circulation due to the hepatic uptake by scavenger receptors of the non-parenchymal cells (Takakura and Hashida 1996).

In this study, the combinational formulation of the pDNA- and DPc-incorporated micelles was used in the PCI-mediated transfection. Polymeric micelles, of which the drug-loaded core is covered with a dense and hydrophilic PEG palisade, are characterized by their small size (less than 100 nm), excellent biocompatibility and stability in biological media (Kataoka et al. 1993, 2001; Nishiyama and Kataoka, 2006). We have so far demonstrated that polymeric micelles incorporating antitumor drugs can stably circulate in the bloodstream and effectively accumulate in solid tumors (Kwon et al. 1994; Nishiyama et al. 2003; Bae et al. 2005). Accordingly, in this study, we have used polymeric micelles as nanocarriers for the pDNA and DPc delivery, expecting their future application in systemic administration. In particular, this paper focused on demonstrating the feasibility of our strategy using the combinational formulation of the pDNA- and DPc-incorporated micelles in the PCI-mediated transfection *in vitro*. In this strategy, both polymeric micelles are assumed to be taken up by the cell through the endocytic pathway and show the same subcellular localization, allowing selective photochemical damaging of the endosomal membrane and effective cytoplasmic delivery of the pDNA-incorporated micelles upon photoirradiation, which might be a key to the successful PCI-mediated transfection. Indeed, the PCI using the DPc-incorporated micelles achieved more than 200-fold photochemical enhancement of the gene transfection of the polyplex micelles. Importantly, the PCI using the combinational micellar formulation achieved a wide range of safe DPc

Table I. Photochemical enhancement of the gene expression and cell viability in the PCI-mediated transfection using each photosensitizer (fluence: 5.4 J/cm^2).

DPc-loaded micelle	DPc conc. (μM)	0.64	0.32	0.16	0.08
	(a) Photochemical enhancement (fold)	72.6 ± 30	211 ± 150*	123 ± 58***	55.7 ± 25
	(b) Cell viability (%)	50.7 ± 1.9	73.8 ± 6.4**	81.2 ± 4.8	86.1 ± 11
DPc	DPc conc. (μM)	0.64	0.32	0.16	0.08
	(a) Photochemical enhancement (fold)	47.1 ± 20	117 ± 16**	64.3 ± 13***	34.2 ± 4.5
	(b) Cell viability (%)	15.7 ± 2.0	18.0 ± 2.3**	73.8 ± 5.8	92.0 ± 4.0
$AlPcS_{2a}$	$AlPcS_{2a}$ conc. (μM)	0.17	0.085	0.043	0.022
	(a) Photochemical enhancement (fold)	8.09 ± 8.9	35.5 ± 8.9*, **	12.9 ± 6.0***	5.63 ± 2.8
	(b) Cell viability (%)	7.15 ± 1.0	15.9 ± 3.7**	37.8 ± 7.8	71.4 ± 3.8

*$P > 0.05$; **$P < 0.01$; and ***$P < 0.05$ ($n = 4$, unpaired t-test).

concentrations and light doses, in which remarkable enhancement of the transfection was achieved without a significant decrease in the cell viability. Such expanded ranges of safe DPc concentrations and light doses should be favorable for the *in vivo* PCI-mediated gene delivery.

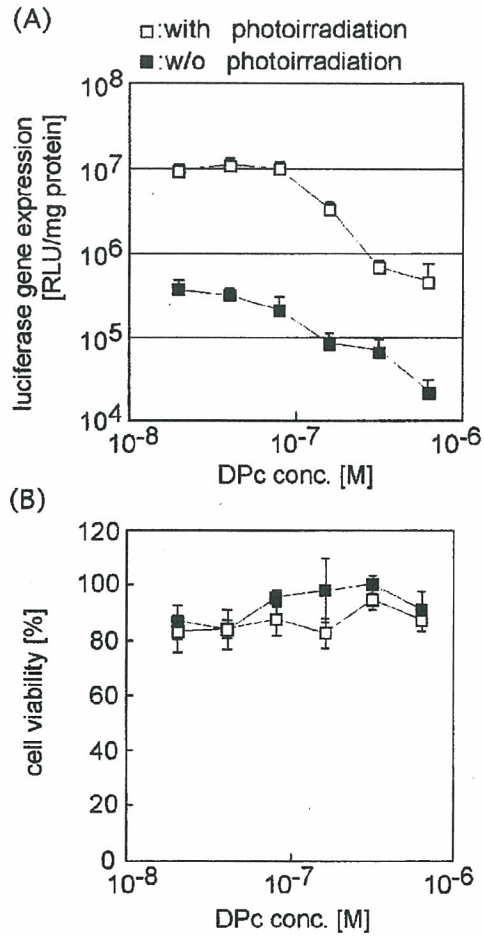

Figure 9. The transfection efficiency (A) and photocytotoxicity (B) in the PCI-mediated transfection using the DPc-incorporated micelles. The light irradiation (fluence: 5.4 J/cm^2) was performed after prolonged incubation (i.e. 24 h) with the pDNA- and DPc-incorporated micelles, followed by 48 h post-incubation in a fresh medium.

In conclusion, polymeric micelles might be a useful nanocarrier, which has been demonstrated to show prolonged blood circulation and thereby accumulate in the target tissues after intravenous administration, motivating us to study the PCI-mediated transfection using the combinational formulation of the pDNA- and DPc-incorporated micelles. Indeed, the PCI using the combinational micellar formulation achieved a remarkable photochemical enhancement of the transgene expression while maintaining an approximately 80% cell viability over a wide range of DPc concentrations and light doses. Thus, the usefulness of our strategy for *in vitro* trasnfection was successfully demonstrated. This system can be potentially useful for the gene therapy of solid tumors and ophthalmic diseases such as age-related macular regeneration (AMD) (Ideta et al. 2005). In addition to therapeutic genes, small interfering RNA (siRNA), which is known as the most powerful tool for sequence-specific silencing of the target genes (Elbashir et al. 2001), might also be delivered in a light-inducible manner by this strategy. The target-selective delivery of the therapeutic genes and siRNA

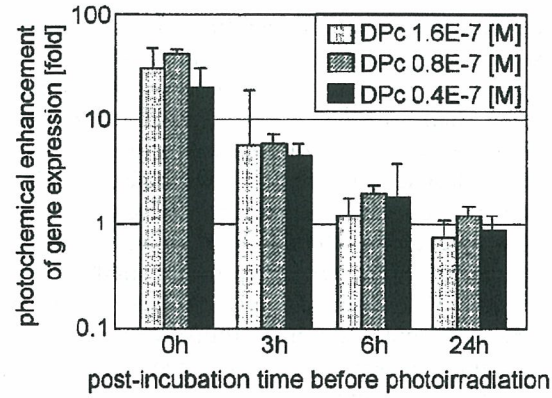

Figure 10. The effect of post-incubation time in the micelle-free medium before photoirradidation on the photochemical enhancement of the transfection of the polyplex micelles in the PCI-mediated transfection using the DPc-incorporated micelles. The cells were photoirradiated (5.4 J/cm^2) at defined post-incubation time after 6 h incubation with the pDNA- and DPc-incorporated micelles and medium replacement with a fresh one, followed by 48 h post-incubation.

by micellar nanocarriers followed by their light-induced activation at the target site might ensure the safety and effectiveness of *in vivo* gene and siRNA therapy. At present, this strategy could be applied only to the tissues, to which a visible light is accessible; however, recent advances in the laser technology such as a two-photon excitation laser (Oh et al. 1997) will solve the problems of limited tissue penetration of the light in the near future. We are now investigating *in vivo* PCI-mediated gene delivery using polymeric micelles via systemic administration and the results will be reported in a forthcoming paper.

Acknowledgements

The authors wish to express their gratefulness to the Health and Labor Sciences Research Grants in Research on Advanced Medical Technology in Nanomedicine Area from the Ministry of Health, Labor and Welfare (MHLW), Japan. Also, they wish to express their thanks for the Grant-in-Aid for Scientific Research, the Special Coordination Funds for Promoting Science and Technology and the Project on the Materials Development for Innovative Nano-Drug Delivery Systems from the Ministry of Education, Culture, Sports, Science and Technology (MEXT), Japan.

References

Bae Y, Nishiyama N, Fukushima S, Koyama H, Matsumura Y, Kataoka K. 2005. Preparation and biological characterization of polymeric micelle drug carriers with intracellular pH-triggered drug release property: Tumor permeability, controlled subcellular drug distribution, and enhanced *in vivo* antitumor efficacy. Bioconjug Chem 16:122–130.

Berg K, Selbo PK, Prasmikaite L, Tjelle TE, Sandvig K, Moan J, Gaudernack G, Fodstad O, Kjølsrud S, Anholt H, Rodal GH, Rodal SK, Høgset A. 1999. Photochemical internalization: A novel technology for delivery of macromolecules into cytosol. Cancer Res 59:1180–1183.

Elbashir SM, Harborth J, Lendeckel W, Yalcin A, Weber K, Tuschl T. 2001. Duplexes of 21-nucleotide RNAs mediate RNA interference in cultured mammalian cells. Nature 411:494–498.

Fukushima S, Miyata K, Nishiyama N, Kanayama N, Yamasaki Y, Kataoka K. 2005. PEGylated polyplex micelles from triblock catiomers with spatially ordered layering of condensed pDNA and buffering units for enhanced intracellular gene delivery. J Am Chem Soc 127:2810–2811.

Harada A, Kataoka K. 1995. Formation of polyion complex micelles in an aqueous milieu from a pair of oppositely charged block copolymers with poly(ethylene glycol) segments. Macromolecules 28:5294–5299.

Harada-Shiba M, Yamauchi K, Harada A, Shimokado K, Kataoka K. 2002. Polyion complex micelles as a vector for gene therapy—pharmacokinetics and *in vivo* gene transfer-. Gene Ther 9:407–414.

Høgset A, Prasmickaite L, Tjelle TE, Berg K. 2000. Photochemical transfection: A new technology for light-induced, site-directed gene delivery. Hum Gene Ther 11:869–880.

Høgset A, Prasmickaite L, Hellum M, Engesæter BØ, Olsen VM, Tjelle TE, Wheeler CJ, Berg K. 2002. Photochemical transfection: A technology for efficient light-directed gene delivery. Somat Cell Mol Genet 27:97–113.

Høgset A, Prasmickaite L, Selbo PK, Hellum M, Engesæter BØ, Bondted A, Berg K. 2004. Photochemical internalization in drug and gene delivery. Adv Drug Deliv Rev 56:95–115.

Ideta R, Tasaka F, Jang W-D, Nishiyama N, Zhang G-D, Harada A, Yanagi Y, Tamaki Y, Aida T, Kataoka K. 2005. Nanotechnology-based photodynamic therapy for neovascular disease using a supramolecular nanocarrier loaded with a dendritic photosensitizer. Nano Lett 5:2426–2431.

Itaka K, Yamauchi K, Harada A, Nakamura K, Kawaguchi H, Kataoka K. 2003. Polyion complex micelles from plasmid DNA and poly(ethylene glycol)–poly(L-lysine) block copolymer as serum-tolerable polyplex system: Physicochemical properties of micelles relevant to gene transfection efficiency. Biomaterials 24:4495–4506.

Itaka K, Miyata K, Harada A, Kawaguchi H, Nakamura K, Kataoka K. 2004. Clinically available endosomolytic agent for gene delivery. In: Svenson S, editor. Carrier-based drug delivery. 879. Washington: ACS Symposium Series. p 154–159.

Jang W-D, Nishiyama N, Zhang G-D, Harada A, Jiang D-L, Kawauci S, Morimoto Y, Kikuchi M, Koyama H, Aida T, Kataoka K. 2005. Suparmolecular nanocarrier of anionic dendrimer porphyrins with PEGylated cationic block copolymer to enhance intracellular photodynamic efficacy. Angew Chem Int Ed 44:419–423.

Kataoka K, Kwon GS, Yokoyama M, Okano T, Sakurai Y. 1993. Block copolymer micelles as vehicles for drug delivery. J Control Release 24:119–132.

Kataoka K, Harada A, Nagasaki Y. 2001. Block copolymer micelles for drug delivery: Design, characterization and biological significance. Adv Drug Deliv Rev 47:113–131.

Katayose S, Kataoka K. 1997. Water-soluble polyion complex associates of DNA and poly(ethylene glycol)–p(L-lysine) block copolymer. Bioconjug Chem 8:702–707.

Kwon GS, Suwa S, Yokoyama M, Okano T, Sakurai Y, Kataoka K. 1994. Enhanced tumor accumulation and prolonged circulation times of micelle-forming poly(ethylene oxide-aspartate) block copolymer–Adriamycin conjugate. J Control Release 29:17–23.

Macdonald IJ, Dougherty TJ. 2001. Basic principle of photodynamic therapy. J Porphyrins Phthalocynanines 5: 105–129.

Merdan T, Kopecek J, Kissel T. 2002. Prospects for cationic polymers in gene and oligonucleotide therapy against cancer. Adv Drug Deliv Rev 54:715–758.

Miyata K, Kakizawa Y, Nishiyama N, Harada A, Yamasaki Y, Koyama H, Kataoka K. 2004. Block catiomer polyplexes with regulated densities of charge and disulfide cross-linking directed to enhance gene expression. J Am Chem Soc 126: 2355–2361.

Moan J, Berg K, Anholt A, Madslien K. 1994. Sulfonated aluminum phthalocyanines as sensitizers for photochemotherapy. Effects of small doses on localization, dye fluorescence and photosensitivity in V79 cells. Int J Cancer 58:865–870.

Ng ACH, Li X, Ng DKP. 1999. Synthesis and photophysical properties of nonaggregated phthalocyanines bearing dendritic substitutes. Macromolecules 32:5292–5298.

Nishiyama N, Stapert HR, Nagano T, Takasu D, Jiang D-L, Aida T, Kataoka K. 2003a. Light-harvesting ionic dendrimer porphyrins as new photosensitizers for photodynamic therapy. Bioconjug Chem 14:58–66.

Nishiyama N, Okazaki S, Cabral H, Miyamoto M, Kato Y, Sugiyama Y, Nishio K, Matsumura Y, Kataoka K. 2003b. Novel cisplatin-incorporated polymeric micelles can eradicate solid tumors in mice. Cancer Res 63:8977–8983.

Nishiyama N, Iriyama A, Jang W-D, Miyata K, Itaka K, Inoue Y, Takahashi H, Yanagi Y, Tamaki Y, Koyama H, Kataoka K. 2005. Light-induced gene transfer from packaged DNA enveloped in a dendrimeric photosensitizer. Nat Mater 4:934–941.

Nishiyama N, Kataoka K. 2006. Nano-structured devices based on block copolymer assemblies for drug delivery: designing structures for enhanced drug function. Adv Polym Sci 193:67–101.

Niwa H, Yamamura K, Miyazaki J. 1991. Efficient selection for high-expression transfectants with a novel eukaryotic vector. Gene 108:193–199.

Ogris M, Wagner E. 2002. Targeting tumors with non-viral gene delivery systems. Drug Discov Today 7:479–485.

Oh DH, Stanley RJ, Lin M, Hoeffler WK, Boxer SG, Berns MW, Bauer E. 1997. Two-photon excitation of 4′-hydroxymethyl-4,5′,8-trimethylpsoralen. Photochem Photobiol 65:91–95.

Pack DW, Hoffman A, Pun S, Stayton PS. 2005. Design and development of polymers for gene delivery. Nat Rev Drug Discov 4:581–593.

Prasmickaite L, Høgset A, Berg K. 2001. Evaluation of different photosensitizers for use in photochemical gene transfection. Photochem Photobiol 73:388–395.

Stapert HR, Nishiyama N, Jiang D-L, Aida T, Kataoka K. 2000. Polyion complex micelles encapsulating light-harvesting ionic dendrimer zinc porphyrins. Langmuir 16:8182–8188.

Takakura Y, Hashida M. 1996. Macromolecular carrier systems for targeted drug delivery: Pharmacokinetic considerations on biodistribution. Pharm Res 13:820–831.

Wakebayashi D, Nishiyama N, Yamasaki Y, Itaka K, Kanayama N, Harada A, Nagasaki Y, Kataoka K. 2004. Lactose-conjugated polyion complex micelles incorporating plasmid DNA as a targetable gene vector system: Their preparation and gene transfecting efficiency against cultured HepG2 cells. J Control Release 95:653–664.

Development of a Fitting Model Suitable for the Isothermal Titration Calorimetric Curve of DNA with Cationic Ligands

Wankee Kim,[†] Yuichi Yamasaki,*[,†] and Kazunori Kataoka*[,†,‡]

Department of Materials Science and Engineering, School of Engineering, The University of Tokyo, 7-3-1 Hongo, Bunkyo-ku, Tokyo 113-8656, Japan, and Center for Disease Biology and Integrative Medicine, Graduate School of Medicine, The University of Tokyo, 7-3-1 Hongo, Bunkyo-ku, Tokyo 113-0033, Japan

Received: December 28, 2005; In Final Form: April 12, 2006

A novel curve fitting model was developed for the isothermal titration calorimetry (ITC) of a cationic ligand binding to DNA. The ligand binding often generates a DNA conformational change from an elongated random coil into a compact collapsed form that is referred to as "DNA condensation". The ligand binding can be classified into two regimes having different binding constants K_i, i.e., the binding to an elongated DNA chain with a binding constant K_1 and with K_2 that occurred during the conformational transition. The two-variable curve fitting models are usually bound by a strict regulation on the difference in the values of the binding constants $K_1 > K_2$. For the DNA condensation, however, the relationships for K_1 and K_2 are still unclear. The novel curve fitting model developed in this study takes into account this uncertainty on the relationship of the binding constants and is highly flexible for the two-variable binding constant system.

Introduction

Isothermal titration calorimetry (ITC) is a useful method to explore the interaction between DNA and cationic ligands.[1−10] By adding a solution of cationic ligands to a DNA solution, the ITC instrument measures the heat accompanied by the binding reaction. The thermodynamic parameters such as changes in enthalpy, entropy, and free energy can be obtained by fitting the ITC curve to an adequate curve fitting model. Nevertheless, general curve fitting models are useful only for simple binding systems, and they may not be applied to particular cases such as DNA condensation.

In general, there are three kinds of curve fitting models, i.e., the single set of identical sites (SSIS) model, two sets of independent sites (TSIS) model, and sequential binding sites (SBS) model.[11,12] The SSIS model satisfies many ligand binding systems when all the binding sites on the substance are identical. The following parameters, stoichiometry N, binding constant K, and change in enthalpy ΔH can be obtained using this fitting model. The TSIS model, which is useful when substances have two kinds of binding sites, enables us to calculate both sets of parameters N_1, K_1, ΔH_1 and N_2, K_2, ΔH_2 for the first and second ligand bindings. While the TSIS model seems to be well adapted to various cases, it should not be applied to the particular system where K_1 is smaller than K_2, because this model is constructed assuming that K_1 is larger than K_2. The SBS model is appropriate for the system, such as the binding of multiple ligands to transition metal ions, for example, the binding of four Br^- ions to Cd^{2+} leading to $CdBr_4^{2-}$. For this case, the number of sequential sites should be integral. The absence of a parameter equivalent to N indicates that the curve fitting is carried out by changing only two parameters, K and H, on each site.

Concerning the binding of cationic ligands to DNA, a conformational change in the DNA chain may affect their binding behavior. The DNA chain collapses after some fraction of negative charges on the phosphate backbone is neutralized by cationic ligands, which is referred to as DNA condensation. The binding process of cationic ligands to DNA can be classified into two parts, a simple binding without a DNA conformational transition and another binding event that followed during the conformational transition. The binding constant for the former is K_1 and that for the latter is K_2. During the beginning of ligand binding, the former binding process proceeds where the DNA chains retain their conformation. Consequently, the latter binding occurs after the former was completed, resulting from the DNA conformational transition.

This scheme is consistent with the prediction of the counterion condensation (CC) theory developed by Oosawa and Manning and with the experimental results obtained from electrophoresis.[13] The CC theory indicates the presence of critical residual charges on elongated DNA chains that results from the former ligand binding. While the degree of charge neutralization depends on the ligand concentration, the critical value of charge neutralization is determined by their valence. For example, the values of DNA in the presence of monovalent, divalent, and trivalent cations are 0.76, 0.88, and 0.92, respectively.[14] Bloomfield concluded that the DNA chains retain their conformation until the degree of charge neutralization is increased to 0.90, indicating that cationic ligands with their valence equal to or grater than 3 possesses the potential to generate DNA condensation. On the contrary, it was clarified that almost all of the negative charges are neutralized in the collapsed state.[15] These experimental results suggest that the DNA conformation and its residual charges correlate with each other, and that the binding manner of the cationic ligands is also affected by DNA conformation. Therefore, the binding classification described above is appropriate for the ligand binding to DNA phosphates.

* To whom correspondence should be addressed: Kazunori Kataoka, tel +81-3-5841-7138, fax +81-3-5841-7139, e-mail kataoka@bmw.t.u-tokyo.ac.jp; Yuichi Yamasaki, tel +81-3-5841-7145, fax +81-3-5841-7139, e-mail yamasaki@bmw.t.u-tokyo.ac.jp.

† Department of Materials Science and Engineering, School of Engineering, The University of Tokyo.

‡ Center for Disease Biology and Integrative Medicine, Graduate School of Medicine, The University of Tokyo.

10.1021/jp057554e CCC: $33.50
Published on Web 05/17/2006

To obtain thermodynamic parameters from the ITC measurements, the suitable fitting model should be carefully chosen by considering the relationship of the magnitude of the binding constants. For the DNA condensation, however, this relationship has so far been unknown. Recently, Teif and Lando theoretically pointed out that the DNA conformational change to the collapsed state takes place when $K_2 > K_1$.[16] Actually, Mel'nikov et al. reported the cooperative binding observed in the transition region of the DNA condensation induced by a cationic surfactant.[17] Thus, we developed a novel fitting model suitable for this situation $K_2 > K_1$ to analyze the binding isotherm obtained from the DNA condensation. In this paper, the binding isotherms obtained from the DNA condensation induced by a low molecular weight condensing reagent, cobalt hexamine ($Co(NH_3)_6^{3+}$), and by a polymeric cation poly(ethylene glycol)−poly(L-lysine) block copolymer (PEG−PLL), are demonstrated as typical examples. The former is treated as a standard chemical of a DNA condensation investigation[18] and the latter as a promising polycation as a gene carrier.[19] A comparison of both binding isotherms and the validity of the novel fitting model will be discussed in detail.

Experimental Section

Materials. The plasmid pGL3 DNA (5256 base pairs) was purchased from Promega (Madison, WI). The plasmid DNA (pDNA) was amplified in competent DH5α *Escherichia coli* and purified using the Qiafilter giga kit (QIAGEN, Germany). A stock solution of pDNA was prepared by dissolving purified pDNA in Millipore grade water containing 10 mM NaCl without any buffer solution. The DNA concentration was determined by the absorption at 260 nm. The PEG−PLL block copolymer with the average PEG molecular weight of 12 000 and the average degree of lysine polymerization of 109 was used in this study. The PEG−PLL block copolymer was prepared as already prescribed.[20] Let us now briefly explain the synthesis. PEG−PLL was synthesized using α-methoxy-ω-amino-PEG to initiate polymerization of the *N*-carboxy anhydride of the *Z*-protected lysine. The length of the lysine segment was regulated by the ratio of the monomer to PEG initiator. The deprotection of lysine was carried out under acidic conditions. ^{1}H NMR and size exclusion chromatography were employed for characterization of this block copolymer. The degree of polymerization is deduced by the ratio of the methylene proton of PEG to that on the lysine residue. Cobalt(III) hexamine trichloride was obtained from Wako Pure Chemicals (Osaka, Japan) and used as received.

Isothermal Titration Calorimetry. Isothermal titration calorimetry (ITC) was performed using a Microcal VP-ITC calorimeter (Northampton, MA) with the normal cell (1.4643 mL) at 30 °C. Two milliliters of pDNA solution (0.3 mM in phosphate) was poured inside the cell after three rinses with 10 mM NaCl solution. The condensing agents were titrated into the pDNA solutions using an injection syringe. The concentrations of cobalt hexamine and PEG−PLL were chosen to be 1.2 and 3 mM (in lysine unit), respectively. Each titration consisted of a preliminary 1-μL injection followed by 29 subsequent 10-μL injections at 3-min intervals. Control experiments were carried out for both ligands to determine the heats of ligand dilution, because the dilution effect should be subtracted to obtain the heat of binding. Prior to the ligand binding experiments, the calorimeter was verified by carrying out the Tris base protonation reaction with hydrochloric acid ($\Delta H = -13.58$ kcal/mol).

Analysis of ITC Curve. The analysis of the obtained ITC curves was performed using origin software with version 5.0 attached to the instrument. First, the integrated ITC curves were obtained from the raw data of the power change at each injection, using the add-on module for the purpose in the software, and then the fittings of those data to the fitting function developed here were performed to obtain the thermodynamic parameters, using a fitting tool prepared in the software, which was based on the Levenberg−Marquardt nonlinear fitting algorithm.

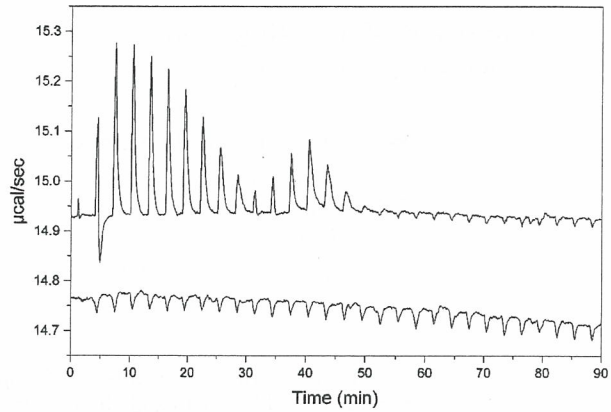

Figure 1. Raw data of ITC measurement for cobalt hexamine binding to plasmid pGL3 DNA in 10 mM NaCl aqueous solution. The upper curve shows the heats resulting from the titration of cobalt hexamine to pDNA solution. The lower curve was obtained by the titration without pDNA, indicating the heats generated by the dilution of the ligand solution. To obtain the ITC binding curves, the lower one should be subtracted from the upper one.

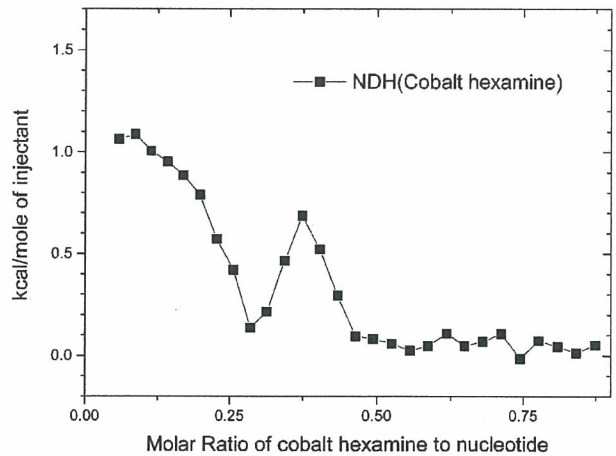

Figure 2. Integrated ITC curve of cobalt hexamine binding to plasmid pGL3 DNA in 10 mM NaCl aqueous solution. This ITC binding curve was calculated from both curves in Figure 1. Endothermic two-stage binding was observed during this ligand binding.

Results

Typical nonintegrated titration curves are shown in Figure 1. The upper curve was obtained by titrating pDNA with cobalt hexamine, and the lower curve was obtained without pDNA indicating the heat of the dilution of cobalt hexamine solution. The upper curve includes the heats resulting from both the dilution effect and the binding reaction. To obtain integrated binding curves as shown in Figure 2, the peaks of both curves were integrated and the latter was subtracted from the former. Figure 2 indicates that the binding of cobalt hexamine onto pDNA can be classified into two stages. Endothermic events were observed during both stages, suggesting that this binding